UNIVERSITY OF CALIFORNIA, SAN DIEGO

A Molecular Characterization of the Role of the Vertebrate Nucleoporin Nup155 in Nuclear Protein Import, Export, mRNA Export, and Nuclear Pore Assembly

A thesis submitted in partial satisfaction of the requirements for the degree Master of Science

in

Biology

by

Steven Walter Martell

Committee in charge:

Professor Douglass Forbes, Chair
Professor Maho Niwa
Professor Ella Tour

2014

The Thesis of Steven Walter Martell is approved, and it is acceptable in quality and form for publication on microfilm and electronically:

Chair

University of California, San Diego

2014

DEDICATION

Without the love and support of my parents, David and Judy Martell, I would be lost. Their unconditional love has been the foundation of who I am today. Knowing that I have the unwavering support of these two is one of the great constants in my life. I am infinitely lucky to have parents who can both share their wisdom with me and be my friend. Their continued emotional and financial support has allowed me to enjoy the best years of my life at UCSD. No words can adequately express my admiration and appreciation. I love you guys so much!

TABLE OF CONTENTS

LIST OF FIGURES

ACKNOWLEDGEMENTS

I would like to graciously thank all of the members of the Forbes lab who have aided my research. Dr. Douglass Forbes is a tremendous resource for all things cell biology, as well as a compassionate, caring friend whose willingness to help knows no bounds. Dr. Boris Fichtman was my initial mentor and taught me the majority of the research techniques that I employ today. His teachings were later carried on by Dr. Cyril Bernis and Michelle Gaylord. Other members of the laboratory, including Beth Swift-Taylor, Salvador Luna, and Matthew Nord have provided me with myriad advice, support, and encouragement. I thank the laboratory of Dr. David L. Spector for providing the Forbes lab with the gift of the p3216PECMS2β plasmid and U20S 2-6-3 cells. Dr. Michal Schwartz and Dr. Anna Travesa-Centrich provided me with specific guidance and advice utilizing this system. My committee members, Dr. Ella Tour and Dr. Maho Niwa-Rosen, have both been gracious advisors to me. Dr. Tour has been an excellent instructor to me for a number of graduate and undergraduate courses. Dr. Niwa-Rosen's frequent presence in the Forbes lab is both uplifting and a solid source for council. I also would like to thank the labs of Dr. James Wilhelm, Dr. James Kadonaga, and Dr. Gentry Patrick for the aid and equipment they have provided over the years. Lastly, I cannot discount the contributions of our faithful custodian Andy; he produces more smiles per day than anybody I know!

ABSTRACT OF THE THESIS

A Molecular Characterization of the Role of the Vertebrate Nucleoporin Nup155 in Nuclear Protein Import, Export, mRNA Export, and Nuclear Pore Assembly

by

Steven Walter Martell

Master of Science in Biology

University of California, San Diego, 2014

Professor Douglass Forbes, Chair

The vertebrate nuclear pore complex is the sole gateway for nuclear-cytoplasmic transport. As it is composed of multiple copies of approximately 30 unique nucleoporin proteins, deciphering the role of each of these is a work in progress. The diverse roles of these proteins have been implicated in countless

cellular processes, including the import and export of proteins, RNA export, mitotic regulation, and cytoskeletal re-arrangement. Here, I have set out to better characterize the role of the scaffold nucleoporin, Nup155. Nup155 is of interest because an R391H mutation has been implicated in atrial fibrillation and early sudden cardiac death in both humans and mice. My work began with an analysis of the localization of wild type and R391H mutant Nup155, as well as their functional domains. Nuclear rim localization was exhibited by WT Nup155 and less so for the α-solenoid and β-propeller domains of WT Nup155. However, neither full length R391H Nup155 nor a R391H β-propeller localized to the nuclear rim. When poly[A]$^+$ mRNA export was assayed, it was found that overexpression of the R391H β-propeller, R391H full length Nup155, and WT β-propeller inhibited export. In contrast, protein import and export through the importin β/exportin-1 pathways were not affected by overexpression of wild type or R391H Nup155. Nor was the actin cytoskeleton affected by overexpression of any of the Nup155 domains or mutants. To determine Nup155 binding partners, a LacI-CFP-Nup155 fusion protein was anchored to a LacO repeat array in the genome. Antibodies to various nucleoporins were used to probe this array. Co-localization of Nup53 and the integral membrane nucleoporin Pom121 revealed that these are likely Nup155 binding partners.

INTRODUCTION

The vertebrate nuclear pore complex (NPC) is a multiprotein complex embedded within the double membranes of the nuclear envelope (NE) (Figure 1a). Nuclear pores mediate all transport between the nucleus and cytoplasm (Tran *et al.*, 2006). This includes both the tightly regulated import of proteins for transcription and DNA replication as well as the export of mRNA and associated proteins. NPCs are composed of approximately 30 different nuclear pore proteins (Nups), which are present in 8, 16, or 32 copies (Alber *et al.*, 2007) (Figure 1b). These Nups make up ~13 soluble sub-complexes. In addition, there are 3 integral membrane proteins (Figure 1b). All are distributed in an eightfold rotational symmetry (Stoffler *et al.*, 1999) (Figure 1b). The entire NPC is 60-125 MDa (Cronshaw *et al.*, 2002). Despite the central role of the nuclear pore complex in a multitude of cellular processes, its overall structure is still a matter of ongoing investigation. In addition, the functionality of the constituent Nups that make up the NPC is also not well characterized. A prime example is the nucleoporin Nup155.

Nup155 has been shown to have a profound impact on nuclear assembly and function. For instance, siRNA depletion of Nup155 from HeLa cells served to both decrease the density of NPCs per unit area and alter the morphology of the nucleus (Mitchell *et al.*, 2010). Similar morphological deformities were seen in siNup155 depleted C. elegans embryos (Mattaj *et al.*, 2005). Additionally, these embryos often featured various deficits in chromosome segregation and in

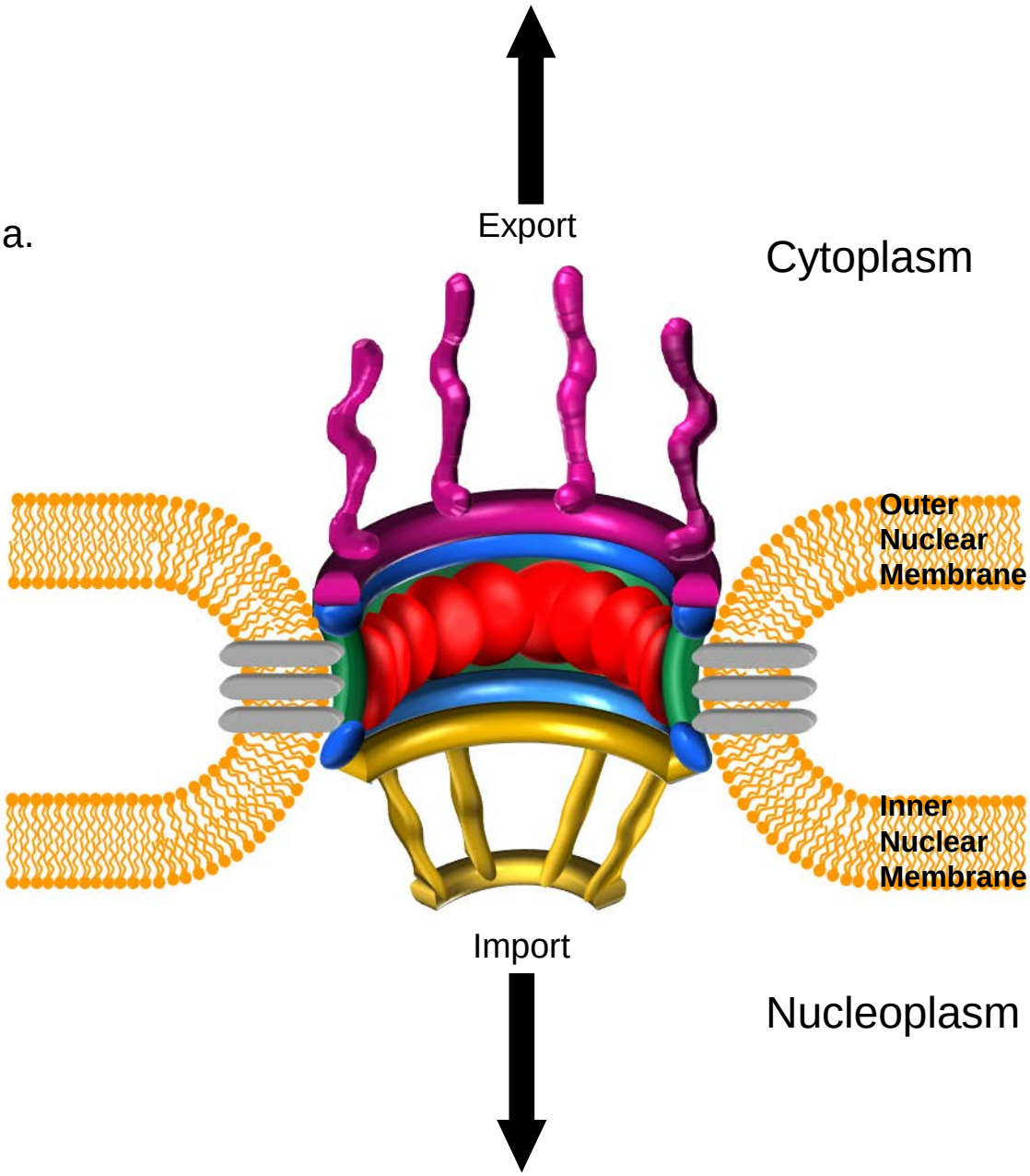

Figure 1 – The Vertebrate Nuclear Pore Complex

(a) An overview cross section of the nuclear pore embedded in the double membranes of the nuclear envelope. (b) 1/8th cross section of the nuclear pore revealing major sub-complexes and general locations of known nucleoporins. Radial symmetry is present along the vertical import/export channel. In (a) and (b), scaffold nucleoporins are shades of blue and green, FG repeat-containing Nups of the central transport channel appear red, cytoplasmic filaments are violet, the nuclear pore basket is gold, and transmembrane nucleoporins are grey.

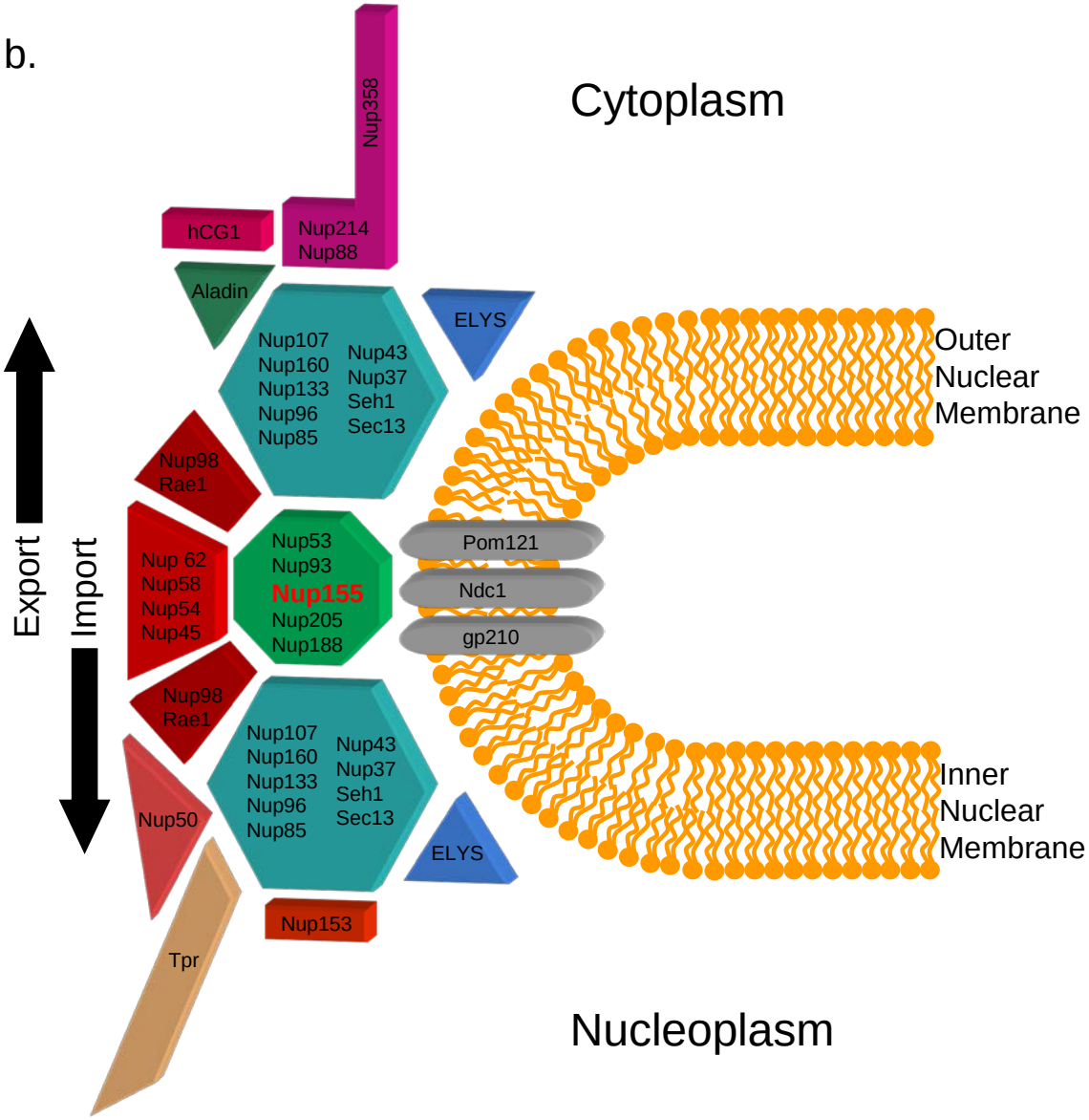

Figure 1, continued

the formation of pronuclei during mitosis (Mattaj *et al.*, 2005). Concomitant with these observations was a mislocalization of other Nups, including Nup358, 153, 98, 53, 93, 107, and Pom121 to cytoplasmic foci and a decrease in the NE localization of inner nuclear membrane (INM) proteins that included Lap2, Lem2, and the lamin B receptor (Mitchell *et al.*, 2010). Furthermore, neither NPCs nor a continuous nuclear membrane were found in a Nup155-depleted Xenopus nuclear assembly reaction (Mattaj *et al.*, 2005). Such results demonstrate the multitude of essential cellular functions related to Nup155.

Here a further investigation into the role of Nup155 was carried out. Protein import into and export from the nucleus by the importin β and exportin-1 pathways was assessed within the context of WT and R391H Nup155. This could help to explain the above deficiencies resultant from Nup155 not being targeted to its correct sub-cellular localization. Export of poly[A]$^+$ mRNA was also examined in the presence of Nup155 fragments, mutations, and wild type protein. Buildup of RNA within the nucleus together with the inability of these transcripts to be read could potentially lead to great consequences (Natalizio and Wente, 2013). The effect of various Nup155 constructs on microfilament structure was also examined. Actin is involved in a multitude of cellular functions including cell division, migration, disease, transcription, and gene expression (Zheng *et al.*, 2009; Huber *et al.*, 2013; dos Remedios and Chhabra, 2008). A more global view of how Nup155 functions in all of these processes should help to explain how this protein is implicated in such disparate cellular functions.

Another aspect of this thesis is a better determination of Nup155-binding partners within the nuclear pore. Nup155 is a component of the core scaffolding of the central ring of the NPC. Previous work on determining Nup155 binding proteins focused on in vitro analysis, mostly involving pulldowns and immunoprecipitations of Nup155 to determine binding partners (Busayavalasa *et al.*, 2012, Hawryluk-Gara *et al.*, 2005, Hawryluk-Gara *et al.*, 2008, Mitchell *et al.*, 2010, Yavuz *et al.*, 2010). Here, in order to elucidate Nup155-interacting Nups under more physiological conditions, we have employed a binding assay system that makes use of a LacI-LacO interaction *in vivo*. In this system, a LacI-CFP-hNup155 chimeric protein was constructed. When expressed it binds to chromatin through the LacI binding to its LacO DNA binding site that has been inserted into the genome. Nup155 binding partners were tested for by looking for co-localization of other nucleoporins using immunofluorescence. A diverse array of Nups from diverse nucleoporin subdomains were chosen to be probed (Figure 1a, 1b for all succeeding examples). Nup160 and Nup133 were selected because they are from the Nup107-160 complex, which constitute the cytoplasmic and nuclear rings of the nuclear pore scaffolding. The Nup107-160 complex is the largest of all pore sub-complexes. In contrast, Nup62 is present in a subcomplex of central Nups that contain phenylalanine-glycine (FG) repeats, known to interact with shuttling nuclear transport receptor proteins, karyopherins. Pom121 was chosen because it is a transmembrane nucleoporin that anchors the NPC to the NE. Nup98 was chosen as it is a peripheral FG-containing Nup present on both the nuclear and cytoplasmic side of the nuclear envelope.

Nup214 is also a peripheral FG Nup, although it is only present on the cytoplasmic side of the pore. Nup93 and Nup53 were selected as they are part of the Nup93-205 complex that comprises part of the central spoke ring of the NPC scaffolding. Interestingly, this is the same complex that contains Nup155. By examining a diverse array of nucleoporins under physiological conditions, we predict that a more complete and accurate survey of Nup155 interactions could be acquired.

Structurally, Nup155 itself can be broken down into 2 major functional domains. These are a ~450 amino acid N-terminal β-propeller domain and a ~591 amino acid C-terminal α-solenoid domain, connected by a ~200 amino acid linker region (Devos *et al.*, 2006). Some experiments using one of the two yeast homologues of Nup155, Nup170, have shed some light on the potential functions of these fragments. In the past, overexpression of the α-solenoid domain lead to incorrect localization of the fragment to the cytoplasm instead of the nuclear rim and was toxic to yeast cells (Flemming *et al.*, 2009). Overexpression of the β-propeller domain was less toxic but did target to nuclear pores, indicating that it serves as the portion of the protein that binds to other Nups (Flemming *et al.*, 2009).

A deeper understanding of Nup155 is desirable as this protein is implicated in a variety of diseases. As the nuclear pore is quite large and contains many different proteins, it is difficult to determine their function. When a nucleoporin is implicated in a disease, much can be learned from the resultant phenotypes. For example, 6% of patients suffering from T-cell acute

lymphoblastic leukemia express a constitutively active Nup214-Abl1 fusion protein kinase (De Keersmaecker *et al.*, 2013). It was discovered that Nup155 binds to this protein in human T cell acute lymphoblastic leukemia (ALL-SIL) cells (De Keersmaecker *et al.*, 2013). Upon siNup155 treatment of these cells, proliferation and viability decreased dramatically, thus opening the door for consideration of therapeutics targeting the nucleoporin Nup155 (De Keersmaecker *et al.*, 2013). Another therapeutic Nup155 application involves p53-mutated B-cell chronic lymphocytic leukemia (CLL). Hsp90 has been found to be over-expressed in such cancers and the synthetic Hsp90 inhibitor SNX-7081 is highly effective at decreasing viability of the CLL cell line, MEC1 (Hertlein *et al.*, 2010; Che *et al.*, 2013). A consequence of SNX-7081 treatment is a > 2-fold decrease in Nup155 protein and mRNA levels (Che *et al.*, 2013). The role of Nup155 in CLL is still unknown, but it is of interest that it is a potential downstream target of a promising anti-cancer therapy.

Another intriguing disease finding with respect to Nup155 concerns an arginine to histidine mutation, R391H, in the β-propeller of Nup155 that leads to atrial fibrillation and sudden early cardiac death in mice (Zhang *et al.*, 2008). The authors described a number of negative phenotypes that are resultant from this mutation. These include the mislocalization of mutant R391H Nup155 transiently transfected into COS7 cells and reduced nuclear envelope permeability in similarly transfected HeLa cells (Zhang *et al.*, 2008). Interestingly, inhibition of Hsp70 mRNA export from the nucleus was observed, as was reduced Hsp70 protein import into the nucleus in HeLa cells (Zhang *et al.*, 2008). Relevant to

this, one source of atrial fibrillation in humans was found to result from a R391H mutation of Nup155 (Zhang *et al.*, 2008). The effects of this mutation on cells expressing both full length and the β-propeller of Nup155 will be evaluated further in the current study.

MATERIALS AND METHODS

Cell Culture

Cells were cultured at 37°C and 5% CO_2 in complete Dulbecco's modification of Eagle's medium (Cellgro) supplemented with 10% FBS, 100 Units / ml penicillin, and 100 μg / ml streptomycin. During transfections, cells were grown in complete Dulbecco's modification of Eagle's medium supplemented with 10% FBS at 37°C. The cells used were HeLa cells, HeLa RGG 2.2 cells (a kind gift from the lab of John Hanover Lab), U20S cells (a kind gift from the lab of David Spector), and U20S 2-6-3 cells (Spector Lab).

Localization Assay

HeLa cells were seeded on coverslips for ~24 hours and then transiently transfected with pCS2+GFP-C1 vectors encoding GFP, xNup155, R391H xNup155, xNup155 β-propeller (a.a. 1-721), R391H xNup155 β-propeller, or xNup155 α-solenoid (a.a. 824-1389) using Lipofectamine 2000 Transfection Reagent (Invitrogen). After ~24 hours of growth, the cells were fixed (3% formaldehyde in PBS, 30', RT), permeabilized (0.1% Triton X-100 in PBS, 5', RT), and blocked (5% nonfat milk in PBS, 30', RT). Primary antibody used to detect FG-containing nucleoporins was mouse anti-414 antibody (1:100 in PBS + 5% nonfat milk, 30', RT). A secondary Alexa Fluor 555-labeled goat anti-mouse antibody was then applied (1:100 in PBS + 5% nonfat milk, 30', RT). Coverslips were mounted on Vectashield with DAPI (2.5 μl, Vector Laboratories) and sealed

with nail fortifier (New York Color). Visualization was carried out with a Zeiss AxioCam HRc camera mounted on a Zeiss Axioskop 2 microscope. Fluorescence intensity analysis in Figure 3 was performed with the "plot profile" tool in ImageJ (Wayne Rasband, National Institute of Health) along a straight line that twice transects the nuclear rim (see Figure 3).

Poly[A]$^+$ mRNA Accumulation Assay

To detect poly[A]$^+$ mRNA accumulation cells were assayed similar to Vasu *et al.*, 2001. HeLa cells were grown on coverslips for 24 h, then transiently transfected for 24 h with myc-tagged hNup160$_{317\text{-}697}$ in pcDNA 3.1a or with GFP-tagged constructs in pCS2+GFP-C1 using jetPEI (Polyplus-transfection). These cells were then fixed (3% formaldehyde in PBS, 20', on ice), permeabilized (0.5% Triton X-100 in PBS, 10', on ice), washed with PBS + 1 mM vanadyl ribonucleoside complexes to inhibit RNAse activity (VRC; New England Biolabs, 5', on ice), incubated with 2X SSC + 1 mM VRC (0.3 M NaCl, 0.03 M sodium citrate, pH 7, 5', on ice), blocked with 10 mg/ml yeast tRNA, 2X SSC, 10% dextran sulfate, 50% formamide, 1 mM VRC, and 1% BSA (1 h, 37°C). Cells were then hybridized with 50 pg/μl oligo dT$_{50}$-Cy3 in the same buffer (16 h, 37°C), washed 3X in 2X SSC (5', 37°C each), then re-fixed (3% formaldehyde in PBS, 15', RT). Myc-hNup160$_{317\text{-}697}$-transfected cells were blocked with 5% FBS in PBS (15', RT) and detected with FITC anti-myc antibody in 5% FBS in PBS (1:200; Santa Cruz Biotechnology, 45', RT). Coverslips were mounted on

Vectashield stained with DAPI (1.0 μl, Vector Laboratories) and sealed with nail fortifier.

RGG Protein Import and Export Assays

HeLa RGG 2.2 cells were grown on coverslips for 24 h, then transiently transfected for 24 h with myc-hNup160$_{317\text{-}697}$ in pcDNA 3.1a or full length xNup155 constructs in pCMV-Sport6p using jetPEI (Polyplus-transfection). After transfection, cells were either untreated (no Dex; Figure 7) or treated with 1 μM dexamethasone (Calibochem; 1 h, 37°C) in Dulbecco's modification of Eagle's medium supplemented with 10% FBS (+Dex; Figure 7) and the cells were visualized by fluorescence microscopy for nuclear import of the RGG fusion protein. Parallel cells were treated with dexamethasone for 1 h to allow RGG import, washed, then incubated with media lacking dexamethasone (2 h, 37°C) in new wells to allow export (+Dex, -Dex; Figure 7). 4 ng / ml leptomycin b (Sigma-Aldrich) was used as a positive control for inhibition of nuclear export during the 2h, 37°C incubation. Cells were then fixed (3% formaldehyde in PBS, 15', RT), permeabilized (0.5% Triton X-100 in PBS, 10', RT), and blocked (5% FBS in PBS, 30', RT). All incubations and washes were performed with Dulbecco's modified Eagle medium supplemented with 10% FBS. Antibodies used were Alexa Fluor 555-labeled rabbit anti-human Nup155 (1:200 in 5% FBS + PBS, 45', RT) and TRITC-labeled mouse anti-cMyc (1:200 in 5% FBS + PBS, Santa Cruz

Biotechnology, 45', RT). Coverslips were mounted on Vectashield with DAPI (1.0 μl, Vector Laboratories) and sealed with nail fortifier.

Microfilament Morphology Assay

HeLa cells were grown on coverslips for 24h, then transiently transfected for 24h with GFP, xNup155, R391H xNup155, xNup155 β-propeller, R391H xNup155 β-propeller, or xNup155 α-solenoid in pCS2+GFP-C1 using jetPEI (Polyplus-transfection). Cells were then fixed (3% formaldehyde in PBS, 15', RT), permeabilized (0.5% Triton X-100 in PBS, 10', RT), and blocked (5% FBS in PBS, 30', RT). Actin was visualized with rhodamine phalloidin (0.3 U in PBS + 5% FBS, ???, 1h, RT). Coverslips were mounted on Vectashield with DAPI (1.0 μl, Vector Laboratories) and sealed with nail fortifier.

LacO – LacI Protein Binding Assay

U20S 2-6-3 cells were grown on coverslips for 24 h at 37°C in Dulbecco's modification of Eagle's medium supplemented with 10% FBS, 100 Units / ml penicillin, 100 μg / ml streptomycin, and 100 μg / ml hygromycin B (Invitrogen). The cells were then transiently transfected for 48 h with LacI-CFP or LacI-CFP-hNup155 in pSV2 using jetPEI (Polyplus-transfection). The media was exchanged for Dulbecco's modification of Eagle's medium supplemented with 10% FBS 5 hours post-transfection. Next, the cells were fixed (4% paraformaldehyde in PBS, 10', RT), permeabilized (0.2% Triton X-100 in PBS,

10', RT), and blocked (5% FBS in PBS, 1.5 h, RT). Primary antibody used to detect transfected proteins was mouse α-LacI (1:100, Millipore, 20 h, 4°C). Primary antibodies used to detect endogenous nucleoporins were Alexa Fluor 555-labeled rabbit anti-human Nup155 (1:200, 1.5 h, RT), rabbit anti-human Nup214 (1:100, 20 h, 4°C), rabbit anti-human Nup53 (1:250, 20 h, 4°C), rabbit anti-human Nup93 (1:50, 20 h, 4°C), rabbit anti-human Nup160 (1:500, 20 h, 4°C), rabbit anti-human Pom121 (1:125, 20 h, 4°C), rabbit anti-human Nup62 (1:150, 20 h, 4°C), rabbit anti-human Nup98 (1:100, 20 h, 4°C), and Alexa Fluor 555-labeled rabbit anti-human Nup133 (1:300, 20 h, 4°C). The secondary antibodies used were FITC-labeled goat anti-mouse (1:500, 1.5 h, RT) and Texas Red-labeled goat anti-rabbit (1:500, 1.5 h, RT). Cells were washed 3 times (0.05% Triton X-100 in PBS, 3', RT) following primary and secondary antibody application. Coverslips were mounted on 1:1 Vectashield with DAPI:Vectashield (2.0 μl, Vector Laboratories) and allowed to dry for 30' before sealing with nail fortifier.

RESULTS

Localization of the Different *Xenopus* Nup155 Constructs

Our first step in characterizing Nup155 was to determine its sub-cellular localization, which was expected to be nuclear rim associated as a result of integrating to the existing HeLa cell nuclear pores, along with determining the localization of Nup155 fragments and mutated forms. Using the Nup155 gene of *Xenopus laevis*, the GFP-fusion constructs show in Figure 2 were created. These Nup155 fusion constructs were then transiently transfected into HeLa cells and observed with fluorescence microscopy 24 hours later. Co-localization of the constructs with mAb414 (α-FG Nups) was used to indicate presence within the nuclear envelope. A GFP-containing vector was used as a negative control for nuclear rim localization as it is present throughout the cytoplasm and nucleoplasm (Figure 3a). Full length GFP-xNup155 was observed at the nuclear rim with a fluorescence pattern nearly identical to mAb414 (Figure 3b). This pattern is consistent with previous Nup155 localization data (Radu *et al.*, 1993). Full length GFP-R391H *Xenopus* Nup155 failed to be recruited to the nuclear envelope, as was seen for human R391H Nup155 by Zhang *et al.* in 2008 (Figure 3c). This verifies that altering this single residue dramatically alters the localization of *Xenopus* Nup155. This results show that the R391H mutation is effective at abolishing the targeting of Nup155 to the NPC.

Both the β-propeller and α-solenoid domains of Nup155 showed weak targeting to the nuclear envelope (Figure 3d, e). The β-propeller fragment has

Figure 2 - Nup155 Protein Constructs

Schematic representation of different Nup155 protein constructs. (a) cDNA encoding full-length *Xenopus laevis* Nup155 (xNup155) was amplified by PCR from the pCMV-SPORT6-xNup155 vector (accession number BC047162.1). For insertion into the eukaryotic expression vector pCS2+GFP, PCR primers flanking the sequence of interest were designed to contain restriction sites for Sal1 on the 5' end and for Sma1 on the 3' end. The PCR product was then purified, digested by the restriction enzymes cited above, and ligated into pCS2+GFP (previously digested with the same restriction enzymes). (b) The R391H mutation was generated using site-directed PCR mutagenesis [following the manufacturer's protocol – Quick Change Site-Directed Mutagenesis (Stratagene)]. Isolation of the α-solenoid and β-propeller domains were obtained by excision. (c) The β-propeller domain was removed (the α-solenoid domain was kept) using the BglII restriction enzyme. One nucleotide was then removed from the BglII restriction site using the Quick Change Site-Directed Mutagenesis technique (Stratagene) to ensure a correct reading frame. (d) The α-solenoid domain was removed (the β-propeller domain was kept) using the Xcm1 and SmaI restriction enzymes on the 5' and 3' ends, respectively. In both (c) and (d), the vectors were re-ligated using a T4 DNA ligase. (g) Schematic representation of untagged full-length wild type xNup155 (expressed with the original pCMV-SPORT6-xNup155 vector). (h) The R391H mutation in full-length pCMV-SPORT6-xNup155 was created as described in (b). (i) Schematic drawing of the LacI-CFP fusion. The cDNA coding for this construct was previously inserted into the pSV2 vector to generate the pSV2-LacI-CFP plasmid (a generous gift from the Spector Lab). (j) The cDNA coding for *Homo sapiens* Nup155 (hNup155) was cloned into this plasmid downstream of the LacI-CFP sequence. Using the pBluescript-R hNup155 vector (accession number CV024666), the hNup155 cDNA sequence was extracted by digestion using the EcoRI and KpnI restriction enzymes on the 5' and 3' ends, respectively. The digested fragments were subsequently purified and finally cloned into the pSV2-LacI-CFP plasmid (previously digested with the same restriction enzymes). In this figure, GFP is shown in green, CFP in blue, LacI in yellow, the Nup155 β-propeller domain in orange, the Nup155 α-solenoid domain in purple. The linker regions are shown in light blue. When present, the R391H mutation is depicted as a dark red line. The pCS2+GFP vector was used for transfection and expression of GFP-fused xNup155 proteins (or GFP alone as a control) in HeLa cells, as depicted in Figures 3, 4, and 8. The pCMV-SPORT6 vector was used for transfection and expression of unlabeled xNup155 proteins in RGG 2.2 stably-transfected HeLa cells, as shown in Figure 7. The pSV2-LacI-CFP vector was used for transfection and expression of hNup155 (or LacI-CFP alone as a control) in U20S 2-6-3 cells, as depicted in Figure 10.

a. GFP-xNup155

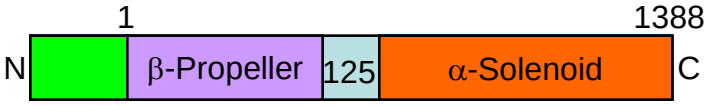

b. GFP-R391HxNup155

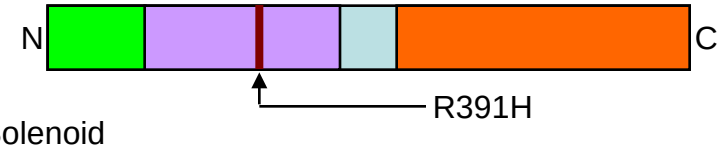

c. GFP-α-Solenoid

d. GFP-β-Propeller

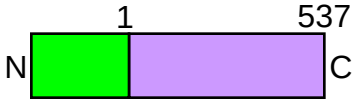

e. GFP-R391H β-Propeller

f. GFP

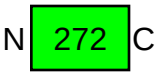

g. xNup155

h. R391H xNup155

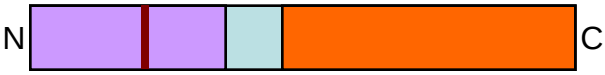

i. LacI-CFP

j. LacI-CFP-hNup155

Figure 3 – Characterization of the Localization of GFP-Tagged Nup155 Wild Type, Functional Domains, and R391H Mutant Forms

HeLa cells were transiently transfected with GFP-tagged fusion constructs of: GFP alone (a), full length xNup155 (b), full length R391H xNup155 (c), the xNup155 α-solenoid domain (d), the xNup155 β-propeller domain (e), or the R391H xNup155 β-propeller domain (f) contained in the pCS2+GFP-C1 vector. Green fluorescence indicates successful transfection of HeLa cells with GFP-tagged Nup155 constructs. The nuclear rim was identified with mouse anti-414 antibody, visualized with Alexa Fluor 555-labeled red goat anti-mouse secondary antibody so as to highlight FG-containing nucleoporins. Nuclei are marked with blue DAPI DNA stain. An ImageJ plot profile tool was used to trace the fluorescence intensity along a line chosen to twice intersect the nuclear rim. The nuclear rim localization of Nup155 (b) is verified by peaks in fluorescence intensity that coincide with FG Nups. This was also observed at a lesser brightness for the α-solenoid (d) and wild type β-propeller (e) constructs. The R391H mutation was found to eliminate nuclear rim localization in both full length (c) and β-propeller (f) constructs.

a.

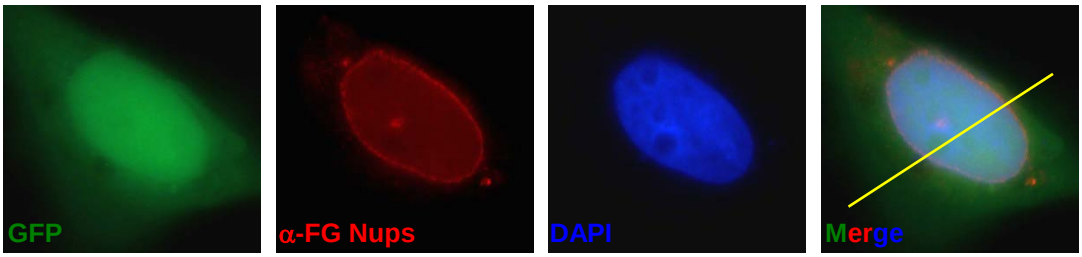
GFP
α-FG Nups
DAPI
Merge

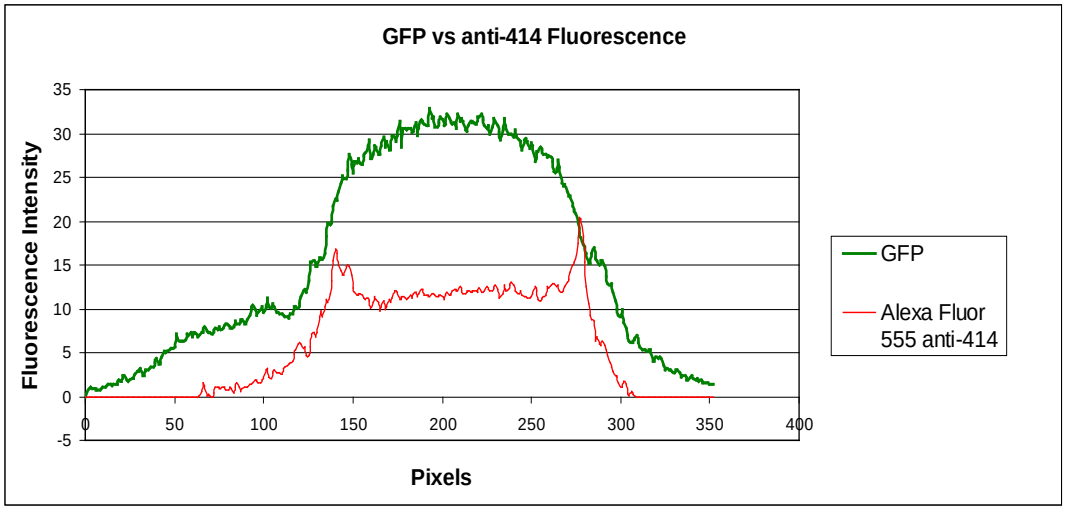
GFP vs anti-414 Fluorescence
Fluorescence Intensity
35
30
25
20
15
10
5
0
-5
0
50
100
150
200
250
300
350
400
Pixels
GFP
Alexa Fluor 555 anti-414

b.

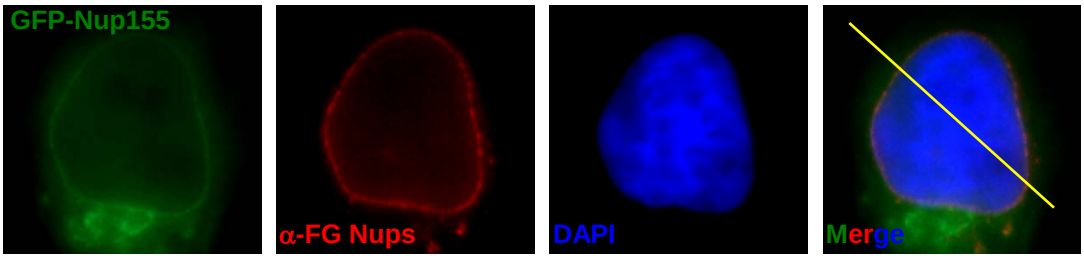
GFP-Nup155
α-FG Nups
DAPI
Merge

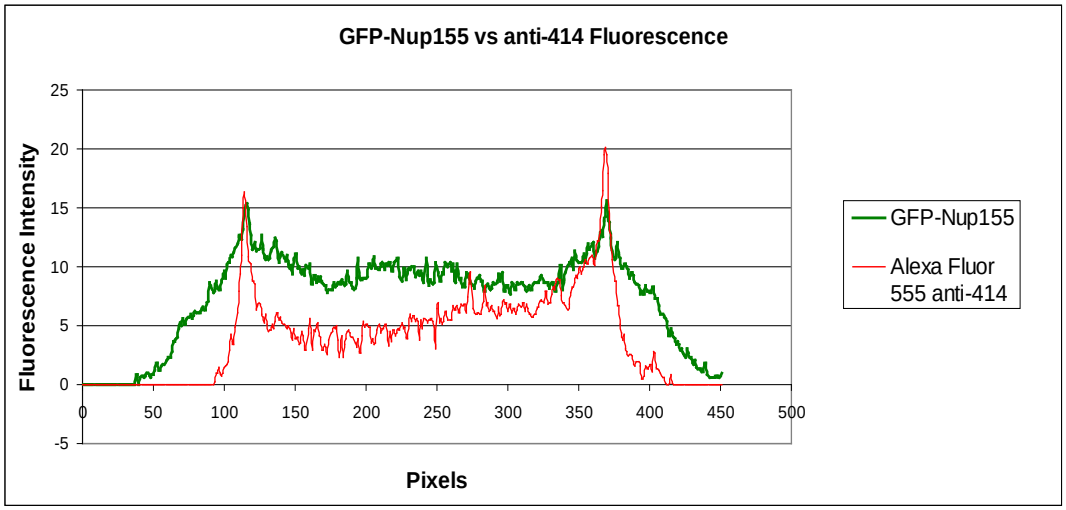
GFP-Nup155 vs anti-414 Fluorescence
Fluorescence Intensity
25
20
15
10
5
0
-5
0
50
100
150
200
250
300
350
400
450
500
Pixels
GFP-Nup155
Alexa Fluor 555 anti-414

c.

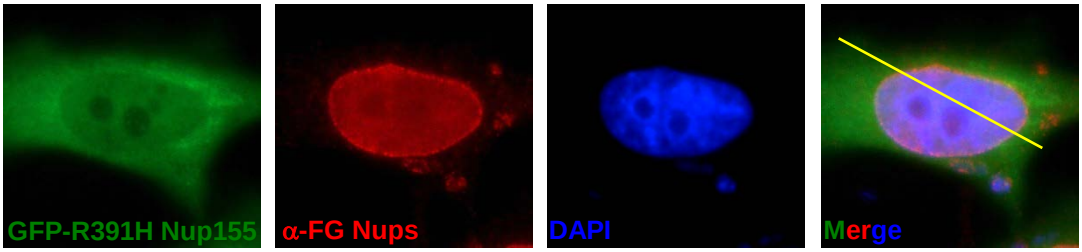

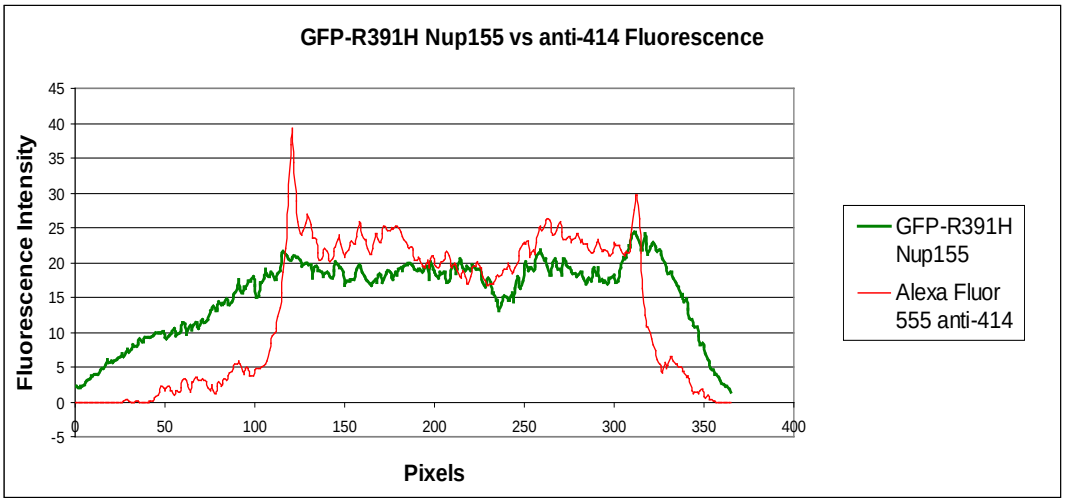

d.

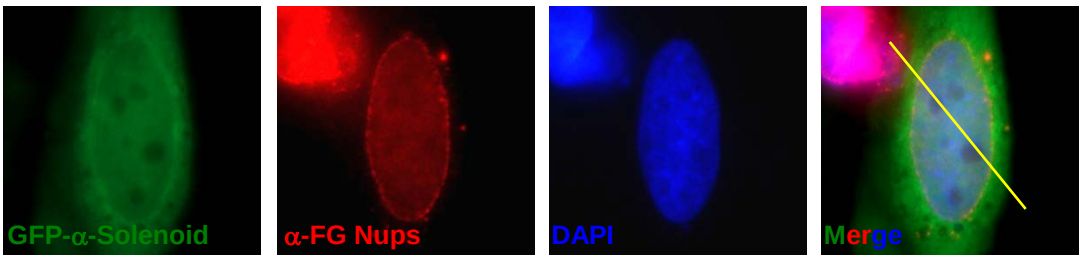

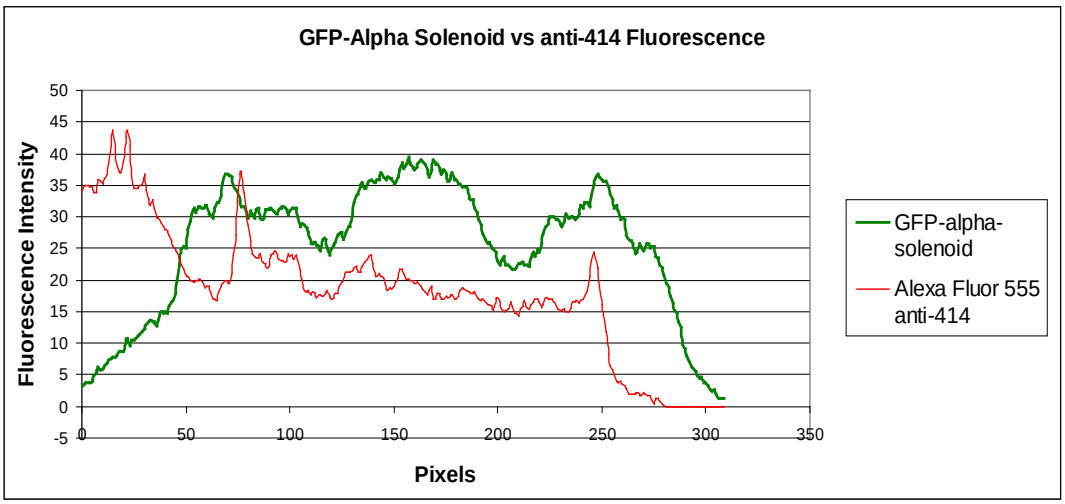

Figure 3, continued

e.

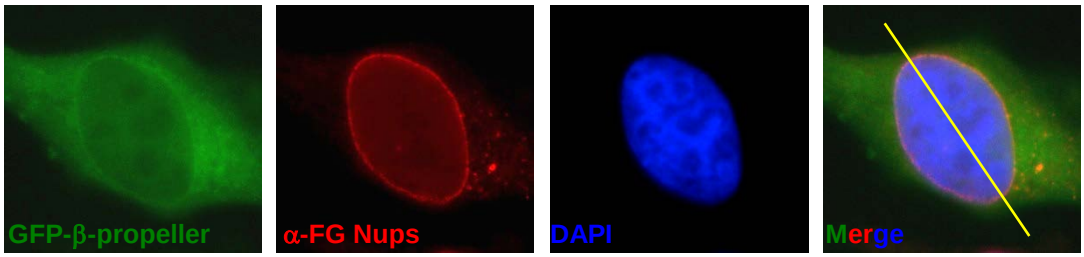

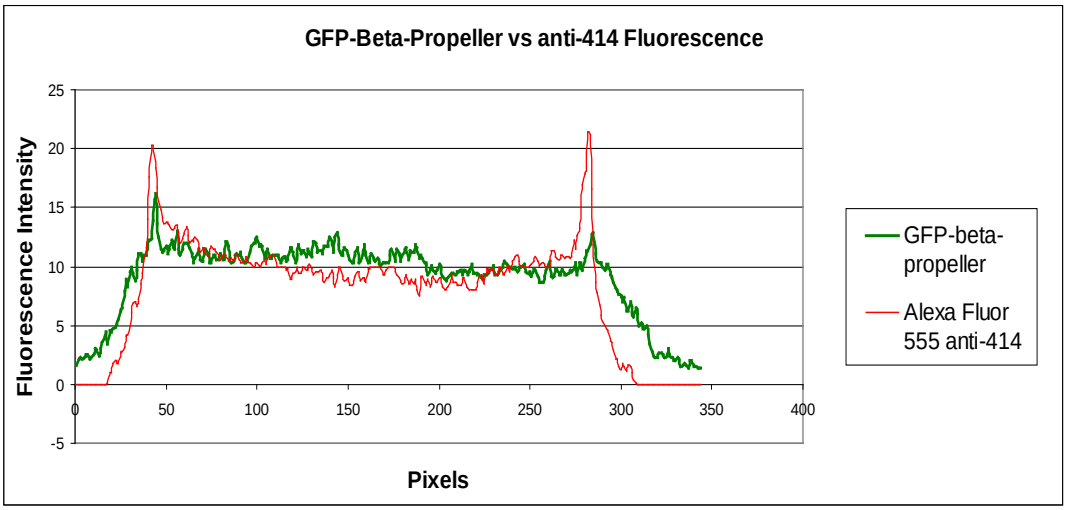

f.

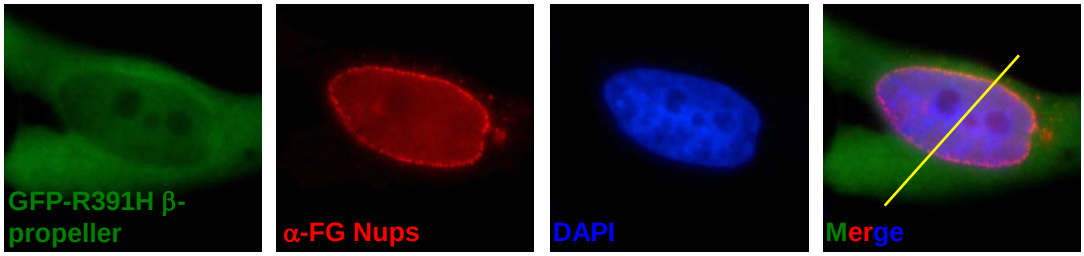

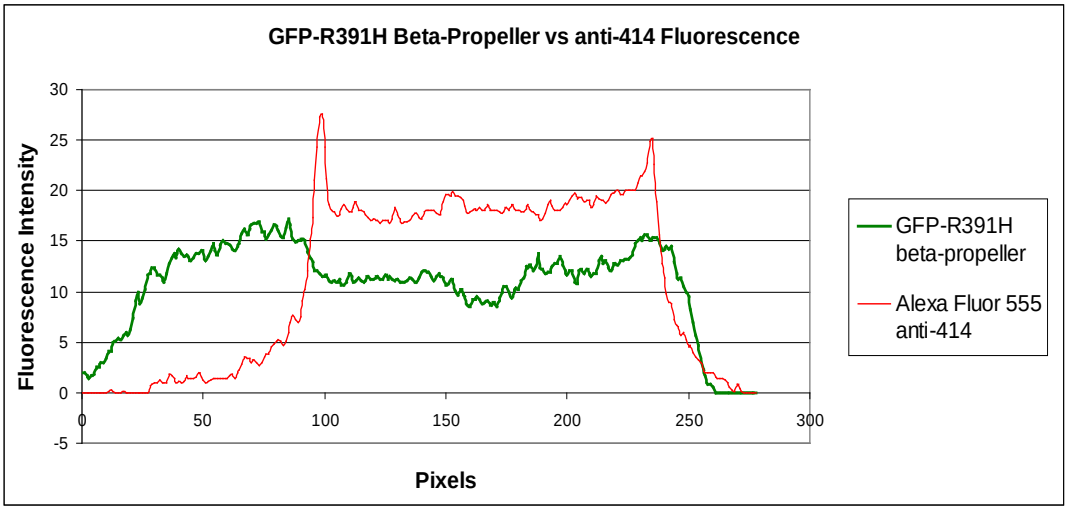

Figure 3, continued

previously been shown to aid in the recruitment of *Drosophila* Nup155 to the NPC in mammalian cells (Busayavalasa *et al.*, 2012). It has also been implicated in anchoring one of the two yeast Nup155 homologues, i.e. Nup170, to the NPC (Flemming *et al.*, 2009). Although the α-solenoid has not been previously show to localize to the pore, it has been implicated in the localization of inner nuclear membrane proteins to the nuclear rim (Busayavalasa *et al.*, 2012). The fact that the *Xenopus* α-solenoid domain was found at the nuclear periphery here could be a result of it's interaction with inner nuclear membrane proteins. The α-solenoid and β-propeller domains could also be working cooperatively to ensure that full length Nup155 is properly recruited to the nuclear pore. Upon transfection, the GFP-R391H β-propeller fusion was not found at the NE, further demonstrating that this mutation blocks nuclear rim association (Figure 3f).

R391H xNup155 and both Wild Type and Mutant Nup155 β-Propeller Domains Inhibit poly[A]$^+$ RNA Export

To discover some of the functional roles of wild type, mutated, and the individual domains of Nup155, an analysis of their role in poly[A]$^+$ mRNA export was undertaken. A 177-amino acid stretch contained within the C-terminal α-solenoid domain of human Nup155 was previously shown to bind to the mRNA export factor human Gle1 (Rayala *et al.* 2004). As hGle1 has been shown to be essential for poly[A]$^+$ RNA export (Watkins *et al.*, 1998), an evaluation of Nup155's role in poly[A]$^+$ RNA export was undertaken here. Of note, the R391H

mutant of human Nup155 was previously shown to inhibit the export of the heat shock protein *Hsp70* mRNA (Zhang *et al.*, 2008). Additionally, when hCG1, a protein that has been shown to directly bind to Nup155, is knocked down with siRNA, a 60-fold increase of Hsp70 mRNA in the nucleus occurred (Kendirgi *et al.*, 2005).

The question being asked here is if this inhibition by R391H Nup155 is of *Hsp70* mRNA, or of all poly[A]$^+$ mRNAs in the cell. This is relevant as *Hsp70* mRNA export occurs through a pathway not normally used by other poly[A]$^+$ mRNA. Most cellular mRNAs are prevented from nuclear export during times of stress (Gallouzi *et al.*, 2000; Krebber *et al.*, 1999; Sadis *et al.*, 1988; Tani *et al.*, 1996). This is not true of the heat shock protein-encoding mRNAs, which are exported at an enhanced rate when heat shock occurs (Bond, 2006; Liu *et al.*, 1996; Saavedra *et al.*, 1996). In fact, *Hsp70* mRNA nuclear export is further facilitated by association of the nuclear basket nucleoporin Tpr with the *HSP70* promoter and *Hsp70* mRNA (Skaggs *et al.*, 2007). The export of *Hsp70* mRNA is thus enhanced during times of heat shock treatment (Skaggs *et al.*, 2007). This leaves us with two potential explanations for the inhibition of *Hsp70* mRNA export after R391H transfection seen by Zhang *et al.*, 2008. One is that the mechanisms needed for export of only heat shock mRNAs is interrupted in mutant R391H Nup155 cells. The other is that a general inhibition of all poly[A]$^+$ mRNA export is occurring both during heat shock and in the absence of heat shock.

Each of the GFP-tagged Nup155 constructs in Figure 2 were transfected into HeLa cells. Poly[A]$^+$ RNA localization was monitored 24 hours later by hybridization to oligo[dT]$_{50}$-Cy3 (Amberg *et al.*, 1992). Cells that were either nontransfected or transiently transfected with GFP alone were used as a negative control (Figure 4a, b). These controls show the typical poly[A]$^+$ RNA stain of diffuse cytoplasmic poly[A]$^+$ RNA staining together with a few brighter intranuclear spots, as is seen in normal cells (Bastos *et al.*, 1996; Heath *et al.*, 1995; Pritchard *et al.*, 1999; Vasu *et al.*, 2001; Watkins *et al.*, 1998). The nontransfected and GFP-transfected cells showed accumulation of poly[A]$^+$ mRNA in the nucleus in only 6.4 $\pm$ 0.3% and 5.1 $\pm$ 0.5% of the cells, respectively (Figure 5). Nup160$_{317\text{-}697}$, a myc-tagged fragment of Nup160, was used as a positive control known to induce poly[A]$^+$ mRNA nuclear accumulation (Vasu *et al.* 2008). Transfection with Nup160$_{317\text{-}697}$ lead to accumulation of poly[A]$^+$ mRNA in the nucleus in 69.9 $\pm$ 1.0% of cells (Figure 4c; Figure 5).

Poly[A]$^+$ RNA accumulation was not particularly enhanced in WT Nup155 or α-solenoid transfection (Figure 4d, f). The percent of accumulating poly[A]$^+$ mRNA after full-length wild type Nup155 or α-solenoid transfection was barely above the negative control baseline, being 11.7 $\pm$ 0.2% and 8.4 $\pm$ 0.1%, respectively (Figure 5). In contrast, transfection of R391H Nup155 and the β-propeller did show noticeably higher levels of inhibited poly[A]$^+$ mRNA export (Figure 4e, g). Such inhibition was seen in 19.9 $\pm$ 1.0% of R391H Nup155-transfected cells, and in 19.6 $\pm$ 0.1% of Nup155 β-propeller transfected cells

Figure 4 – Transfection of full length R391H xNup155 and the Wild Type or R391H xNup155 β-Propeller Domain Inhibit poly[A]$^+$ mRNA Export

HeLa cells were transiently transfected with pCS2+GFP-C1 vectors containing GFP alone (negative control; a), full length xNup155 (d), full length R391H xNup155 (e), the xNup155 α-solenoid domain (f), the xNup155 β-propeller domain (g), or the R391H xNup155 β-propeller domain (h). Transfection with a pcDNA 3.1a vector containing hNup160$_{317-697}$ (c) served as a positive inhibitory control of poly[A]$^+$ RNA export. Successful transfection was assessed by GFP fluorescence of the xNup155 constructs or by FITC-labeled anti-myc antibody used against myc-hNup160$_{317-697}$ (first column). The localization of poly[A]$^+$ mRNA was assessed by hybridization of the coverslips with oligo dT$_{50}$-Cy3 (red; second column). Nuclei are demarcated with blue DAPI DNA stain (third column). A significantly higher nuclear to cytoplasmic ratio of poly[A]+ mRNA was observed upon transfection of R391H Nup155 (e), the wild type Nup155 β-propeller (g), and the mutated R391H β-propeller (h).

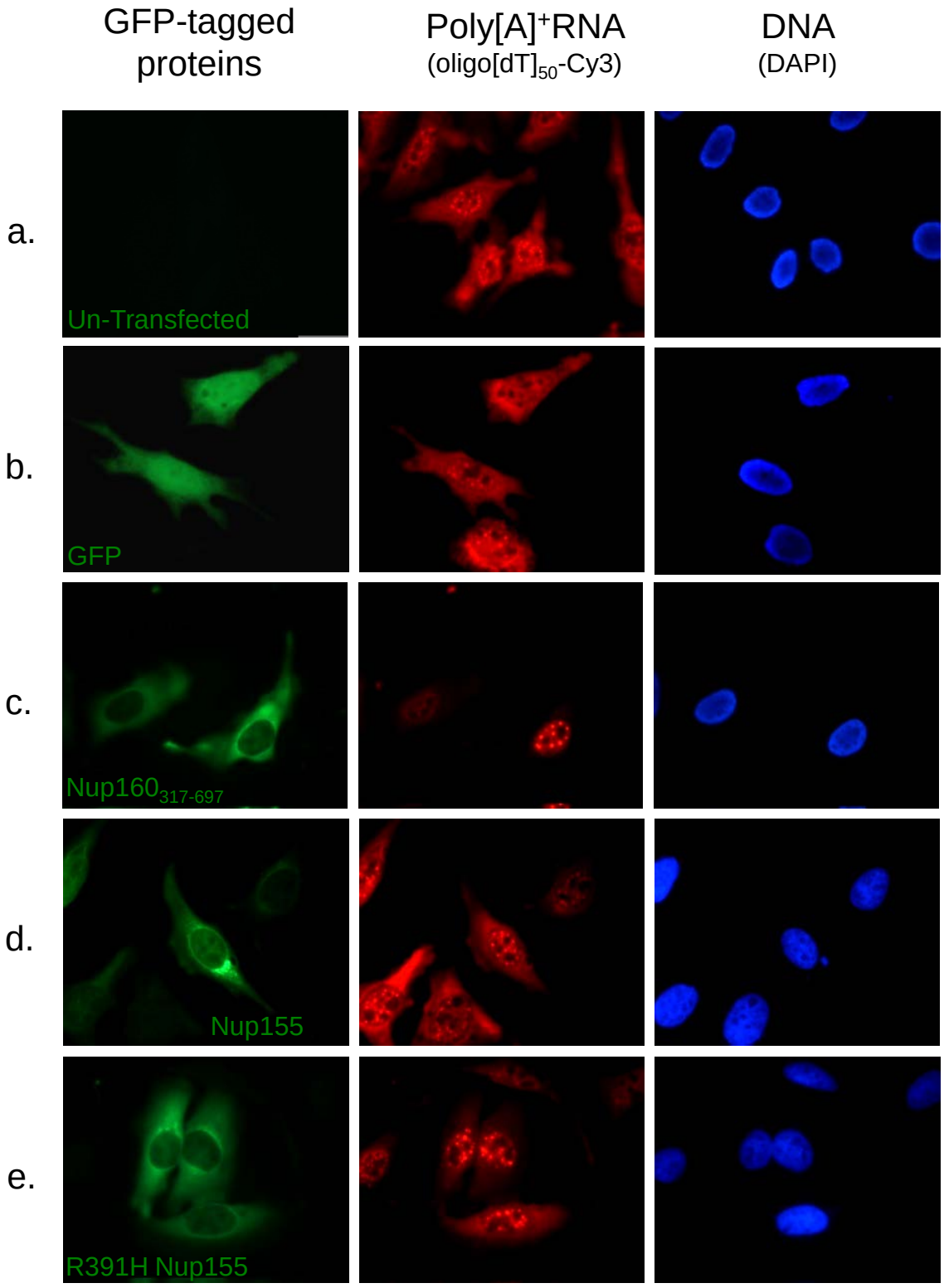
GFP-tagged proteins
Poly[A]+RNA (oligo[dT]50-Cy3)
DNA (DAPI)
a.
Un-Transfected
b.
GFP
c.
Nup160317-697
d.
Nup155
e.
R391H Nup155

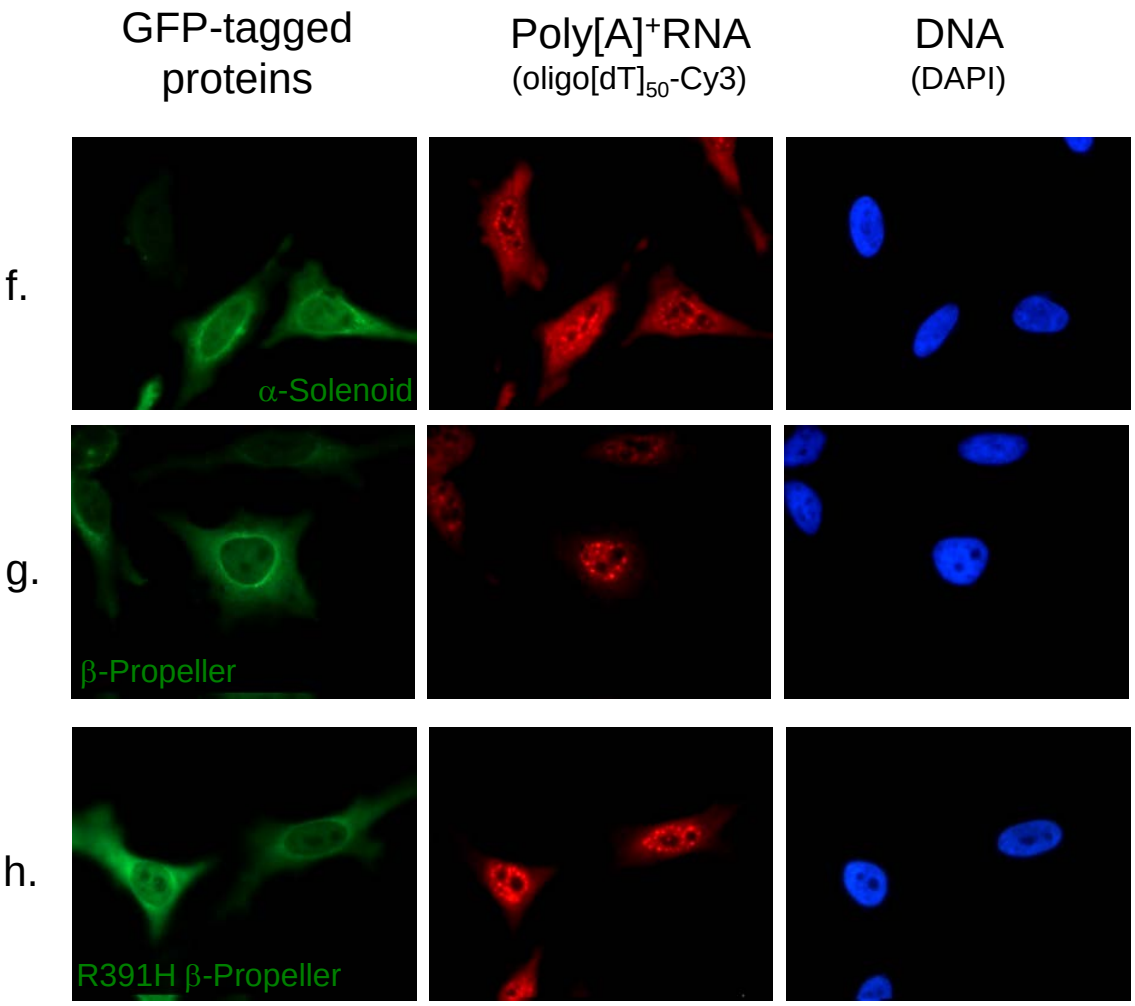

Figure 4, continued

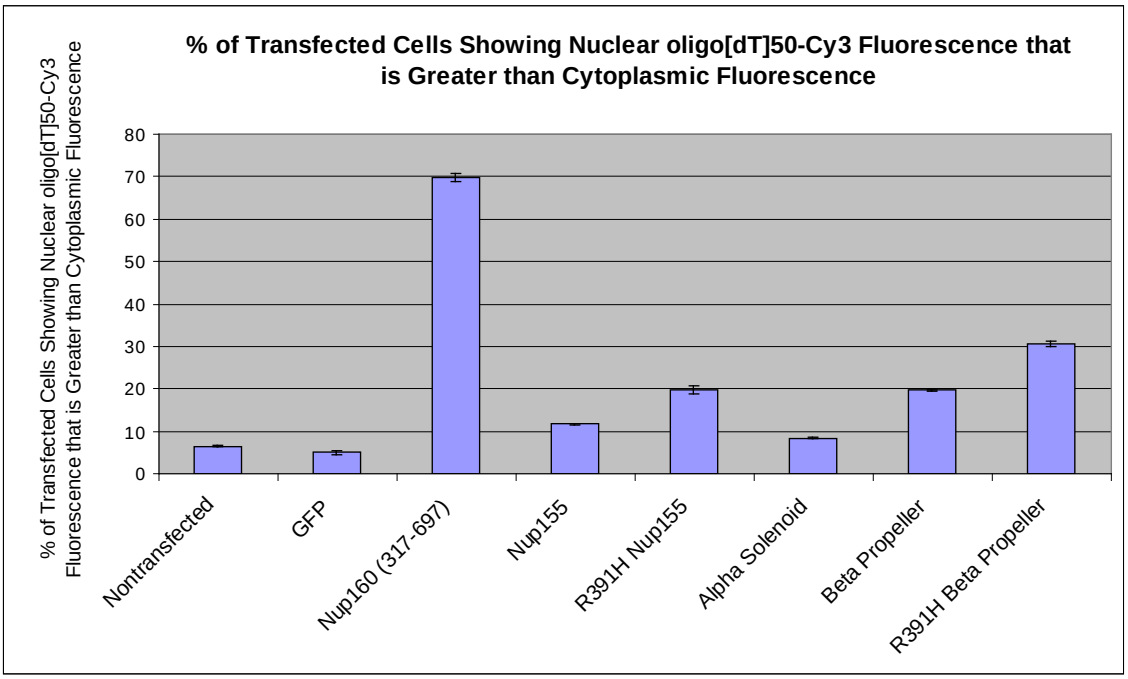

Figure 5 - Quantitation of poly[A]$^+$ RNA Export Inhibition by Nup155 Constructs

HeLa cells transiently transfected with Nup155 constructs in Figure 3 were evaluated for the inhibition of poly[A]$^+$ RNA export. Inhibition was defined by an oligo[dT]$_{50}$-Cy3 fluorescence in the nucleus that is more intense than that of the cytoplasm. At least 150 cell were counted for each condition. Nontransfected and GFP conditions are negative controls; mRNA is successfully exported into the cytoplasm. hNup160$_{317-697}$ fragment shows a profound nuclear retention of poly[A]$^+$ RNA and thus serves as a positive control. Cells transfected with the β-propeller domain, full length R391H Nup155, or the R391H β-propeller domain display a marked increase in nuclear oligo[dT]$_{50}$-Cy3 fluorescence. Error bars represent standard error.

(Figure 5). An even higher level of poly[A]$^+$ RNA accumulation in the nucleus was observed in cells transfected with the R391H β-propeller (Figure 4h). In this case, 30.7 ± 0.7% of R391H β-propeller transfected cells failed to correctly export poly[A]$^+$ mRNA (Figure 5).

Taken together, these results show that the R391H mutation and also the β-propeller have a significant effect on mRNA export. Although none of these proteins had the same effect as Nup160$_{317-697}$, the percentages of cells displaying an inhibition of poly[A]$^+$ mRNA export from the nucleus was compelling enough to infer that Nup155 does play a role in cellular mRNA export. When Nup155 is mutated, a dominant negative effect on total mRNA export is seen. Thus, the effects on inhibition of export by R391H Nup155 reported by Zhang, *et al.* were not confined to the unique process of heat shocks mRNA export, but instead affects all cellular poly[A]$^+$ mRNA.

Nup155 Does Not Have a Role in RGG Protein Import/Export

In order to determine if protein import and/or export from the nucleus is affected by wild type or mutant Nup155 overexpression, the shuttling reporter protein RGG was used (Love *et al.*, 1998). RGG is a fusion protein with 3 major functional components. These are: (1) the nuclear export sequence (NES) from the human immunodeficiency virus (HIV) protein Rev, (2) a hormone-dependent nuclear localization sequence (NLS) from the ligand binding domain of the glucocorticoid receptor, and (3) GFP (Figure 6a) (Love *et al.*, 1998). When stably transfected cells expressing RGG are untreated, the RGG protein is produced

Figure 6 – The RGG Protein Import and Export Assay

(a) The RGG protein is stably expressed by HeLa RGG 2.2 cells. RGG is a fusion composed of 3 constituent domains: (1) The human immunodeficiency virus (HIV) protein Rev. Rev contains both a nuclear localization signal (NLS) for nuclear import targeting and a nuclear export signal (NES) for nuclear export targeting. (2) 2 NLS sequences that are present within the hormone-dependent ligand binding domain of the glucocorticoid receptor. (3) GFP.

In the absence of dexamethasone, a synthetic hormone analogue, that binds to the glucocorticoid receptor, RGG protein localizes in the cytoplasm (b). Upon addition of dexamethasone, RGG protein is imported into the nucleus via the nuclear import receptor, importin β (c). When dexamethasone is washed away with fresh media, the RGG protein is exported out of the nucleus and into the cytoplasm via the nuclear export receptor, exportin-1 (d).

a.

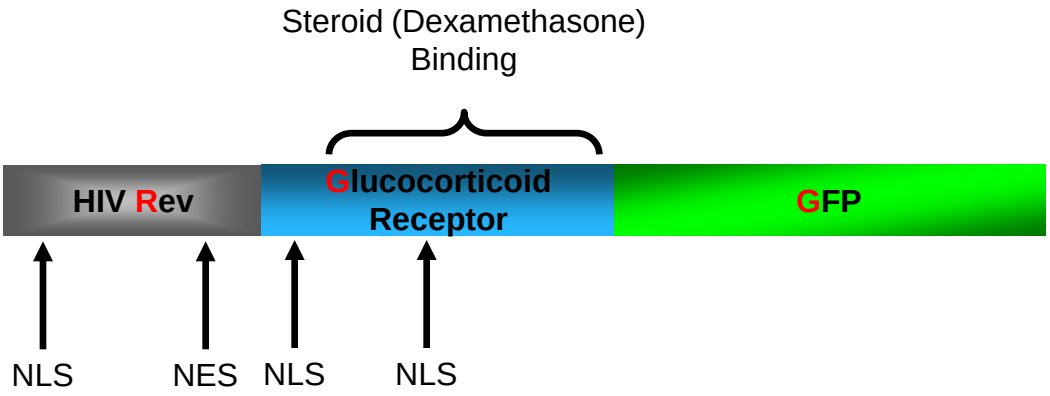

b. No Dexamethasone (No Dex)

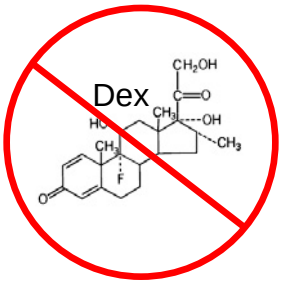

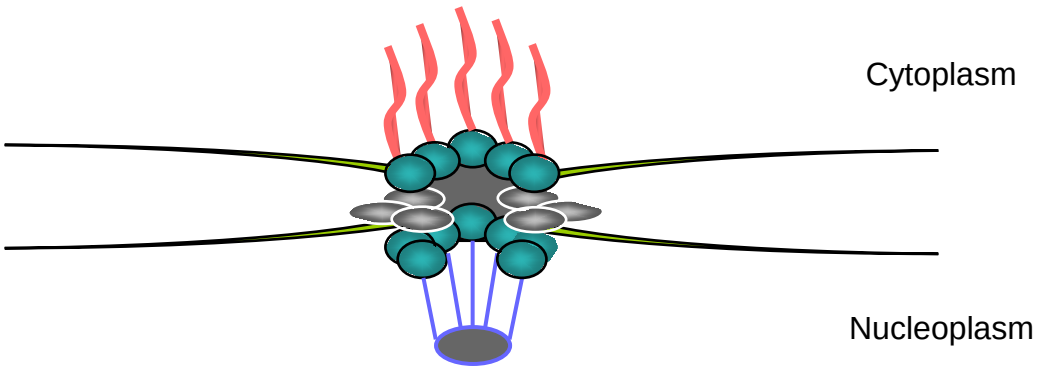

Under wild type conditions, **RGG** is cytoplasmic

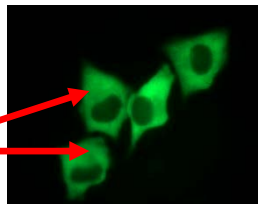

c. 1 μM Dexamethasone (+ Dex)

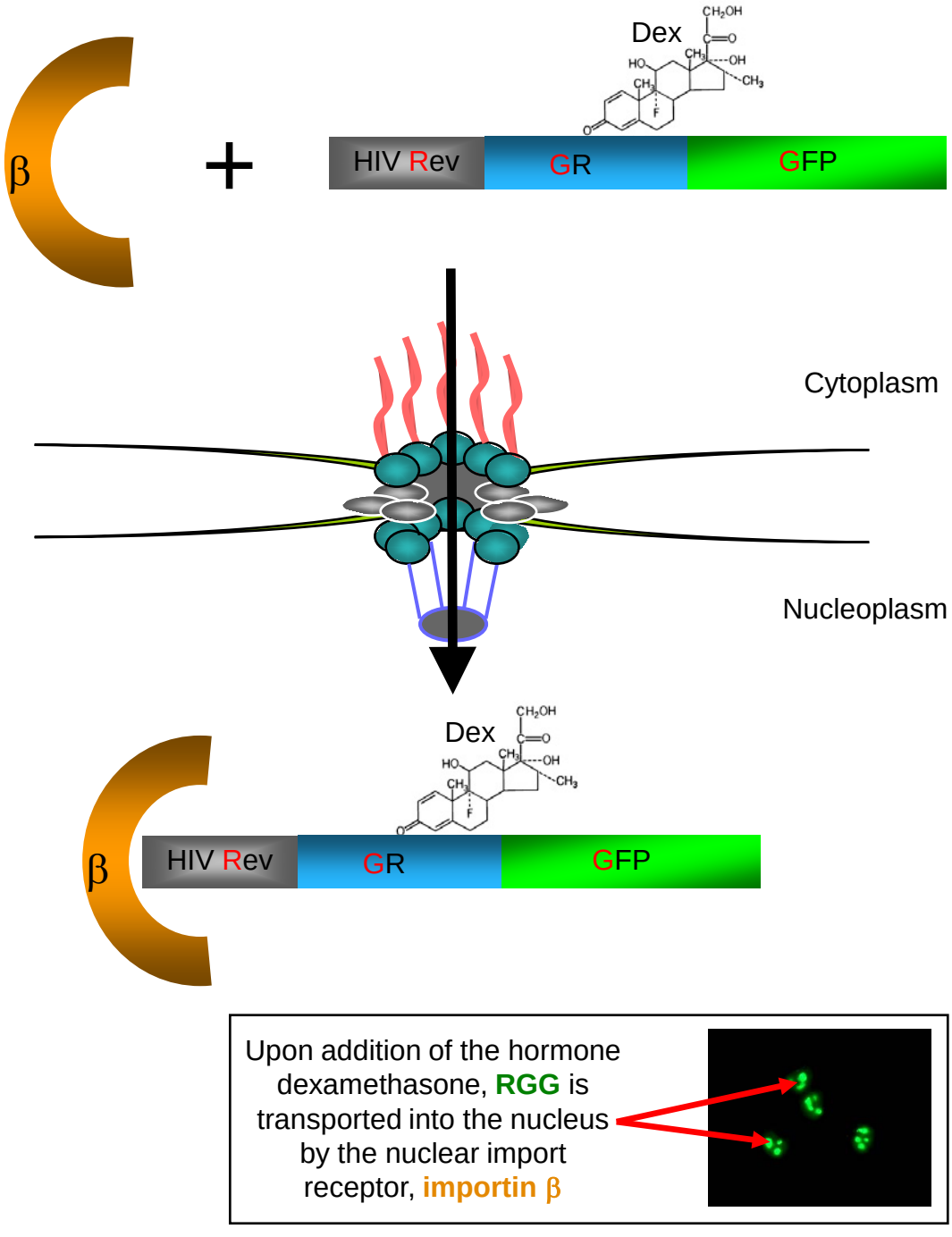

Figure 6, continued

d. 1 μM Dexamethasone, then wash dexamethasone away with media (+ Dex, - Dex)

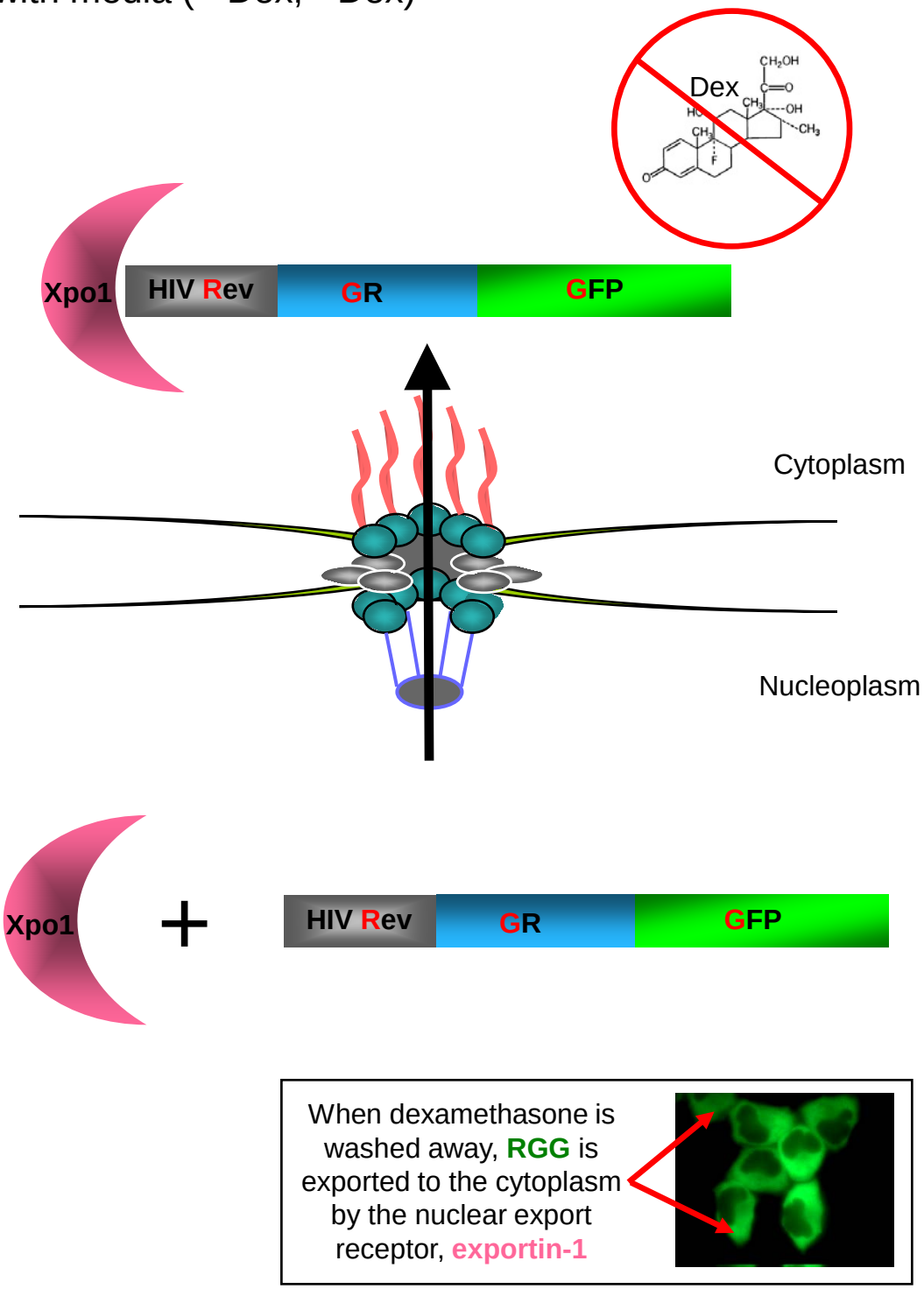

Figure 6, continued

but is localized to the cytoplasm (Figure 6b; Figure 7a, 1st column, no Dex) (Love *et al.*, 1998). When the dexamethasone, a synthetic hormone analogue, is added, this activates the nuclear localization sequence and the RGG protein is imported into the nucleus by the nuclear import receptor importin β (Figure 6c) (Henderson and Percipalle, 1997; Love *et al.*, 1998; Perkins *et al.* 1989). Once inside the nucleus, the RGG protein is known to target to the multiple nucleoli (Figure 7a, 2nd column, +Dex). Transfection by us of wild type Nup155 or R391H Nup155 had no significant effect on RGG protein import (Figure 7d, e, 2nd column, +Dex).

Normally, removal of the dexamethasone is known to lead to the nuclear export of RGG by means of the Crm1/exportin-1 nuclear export receptor (Figure 6d) (Fornerod *et al.*, 1997, Love *et al.*, 1998). This was observed here (Figure 7, 3rd column, +Dex, -Dex). Leptomycin B, an inhibitor of Crm1/exportin-1, was used as a positive control, as it is known to inhibit REV export, blocking RGG in the nucleus (Figure 7c, 3rd column) (Wolff *et al.*, 1997). We found that upon transfection of either WT or R391H Nup155, no inhibition of RGG protein import or export was observed (Figure 7d, e, 3rd column). The effects of these proteins were comparable to that of the Myc-Nup160$_{317-697}$ fragment, which is known to have no negative effect on RGG import and export (Figure 7b) (Vasu *et al.*, 2001). These results demonstrate that the inhibition of poly[A]$^+$ mRNA export observed above with R391H Nup155 transfection is independent of protein import and export through the importin β and exportin-1 pathways.

Figure 7 – Exogenous Expression of Wild Type or R391H xNup155 Inhibits Neither RGG Protein Import or Export

HeLa RGG 2.2 cells stably transfected with RGG protein were transiently transfected with (b) $hNup160_{317-697}$ in pcDNA 3.1a (negative control for inhibited import and export), (d) xNup155 in pCMV-Sport6p, (e) R391H xNup155 in pCMV-Sport6p. (a and c) Non-transfected cells are shown. RGG GFP fluorescence is indicated in green. Anti-Myc TRITC antibodies were used to detect $Nup160_{317-697}$ in red (b). Alexa Fluor 555-labeled anti-Nup155 antibodies were used to detect wild type and R391H Nup155 in red (d and e, respectively). DAPI stain indicates nuclear DNA in blue. After transfection of the test Nup155 or Nup160 constructs, parallel sets of cells were either untreated (no Dex, 1st column), treated for 1 hour with dexamethasone (+ Dex, 2nd column), or treated for 1 hour with dexamethasone, washed, treated for 2 hours with media lacking dexamethasone (+ Dex, - Dex, 3rd column). Leptomycin B (4 ng / ml; positive control for inhibited protein export, c) was added to cells after washing to prevent RGG protein export. Neither Nup155 nor R391H Nup155 had any effect on RGG protein import or export.

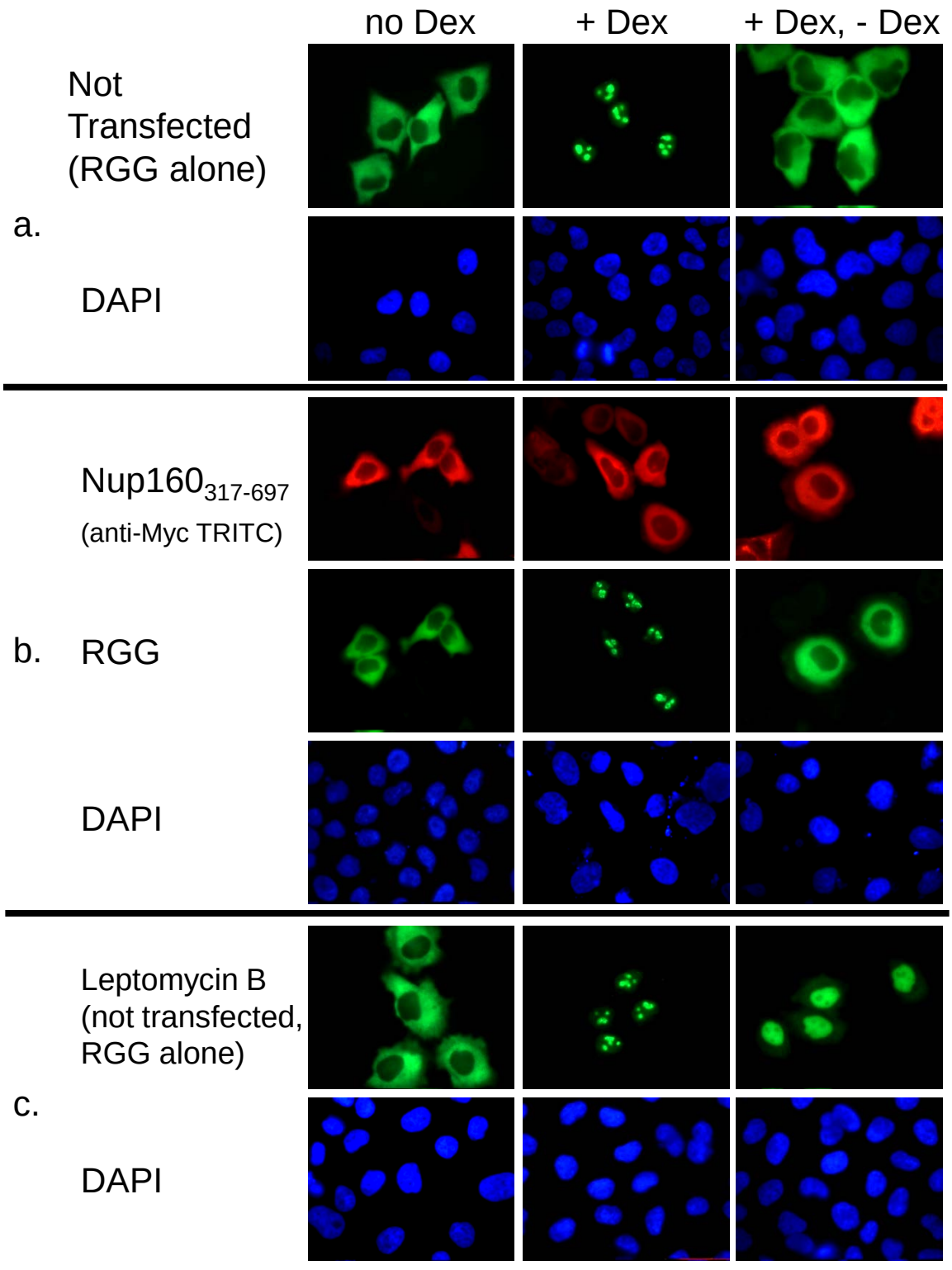
no Dex
+ Dex
+ Dex, - Dex
Not Transfected (RGG alone)
a.
DAPI
Nup160317-697 (anti-Myc TRITC)
b.
RGG
DAPI
Leptomycin B (not transfected, RGG alone)
c.
DAPI

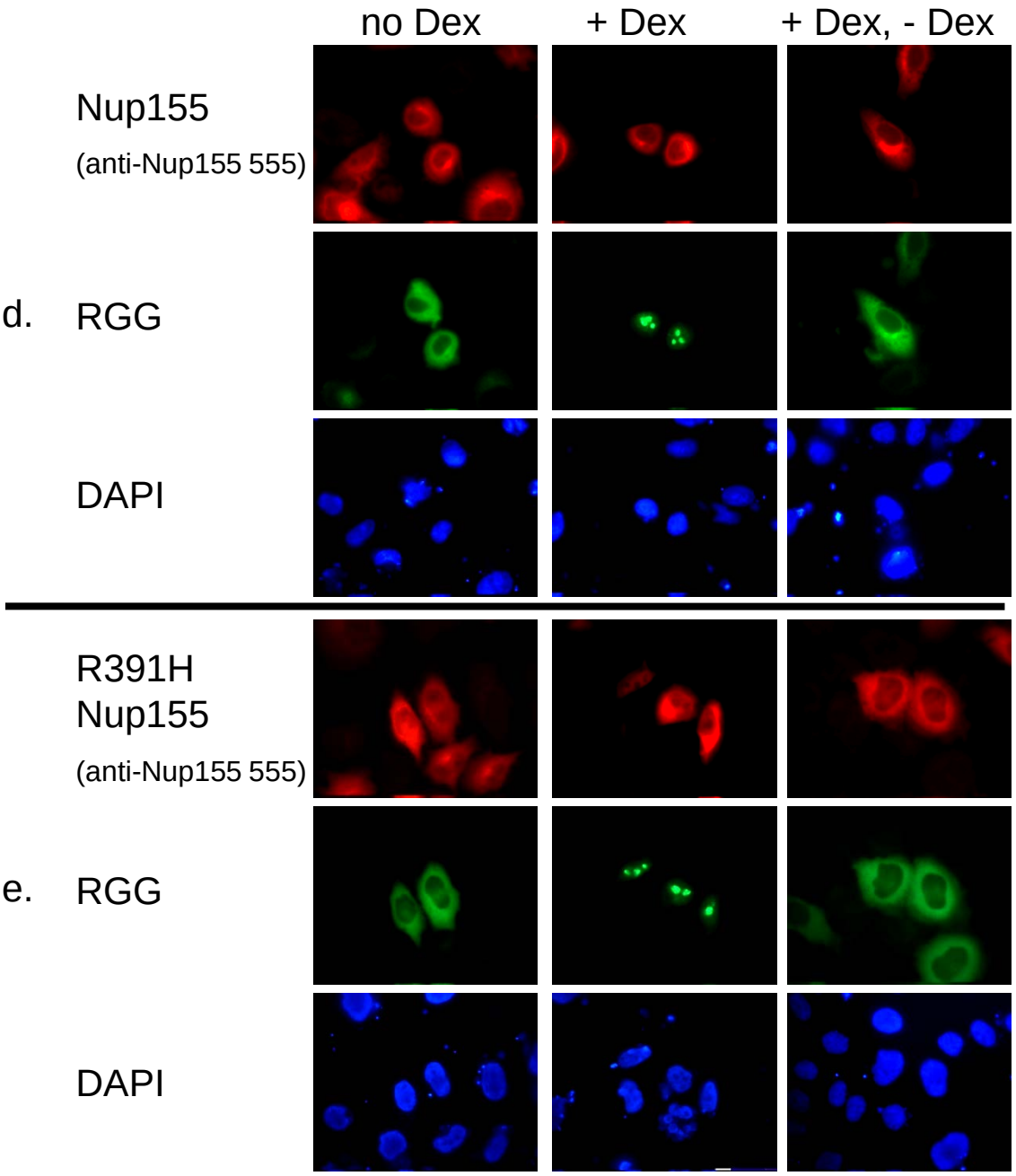

Figure 7, continued

Nup155 Does Not Affect Microfilament Structures in HeLa Cells

Previous studies have shown that depletion of the nucleoporin Nup153, a basket nucleoporin, surprisingly can cause significant alteration of the actin cytoskeletal organization (Zhou and Panté, 2010). HeLa cells depleted of Nup153 by RNAi featured elongated F-actin bundles that contrasted with a more mesh-like network of F-actin in mock depleted cells (Zhou and Panté, 2010). We tested the effect of expression of WT Nup155, R391H Nup155, or the fragments of Nup155 on the actin cytoskeleton by overexpressing these Nup155 proteins in HeLa cells. After transient transfection, actin microfilaments were labeled with rhodamine-phalloidin. By comparing such transfected cells to mock-transfected cells, changes in the actin network could be assessed. However, Figure 8 indicates that no significant morphological alterations resulted from overexpression of any of the tested Nup155 constructs. This implies that the deficiency in mRNA export observed is unrelated to microfilament assembly and that the state of the actin cytoskeleton is completely independent of Nup155.

A LacI – LacO Reporter System Identifies Nup53 and Pom121 as Nup155 Binding Proteins

Most binding assays are conducted *in vitro* using pulldowns or immunoprecipitations. An *in vivo* process, if possible, would be preferred in this situation so that the proteins are exposed to native, physiological conditions. A technique that can overcome these shortcomings is the LacI – LacO reporter system that has been tailored to nuclear conditions (Janicki *et al.*, 2004;

Figure 8 - Nup155 Has No Effect on Actin Morphology in HeLa Cells

HeLa cells were either (a) nontransfected or transiently transfected with pCS2+GFP-C1 vectors containing (b) GFP (negative control), (c) xNup155, (d) R391H xNup155, (e) xNup155 α-solenoid, (f) xNup155 β-propeller, or (g) R391H xNup155 β-propeller. Green GFP fluorescence indicates successful transfection of Nup155 constructs. Actin is labeled with rhodamine-phalloidin (red). Nuclei are marked with blue DAPI DNA stain. No significant changes in the actin cytoskeleton can be observed for any of the Nup155 constructs when compared to GFP or non-transfected controls.

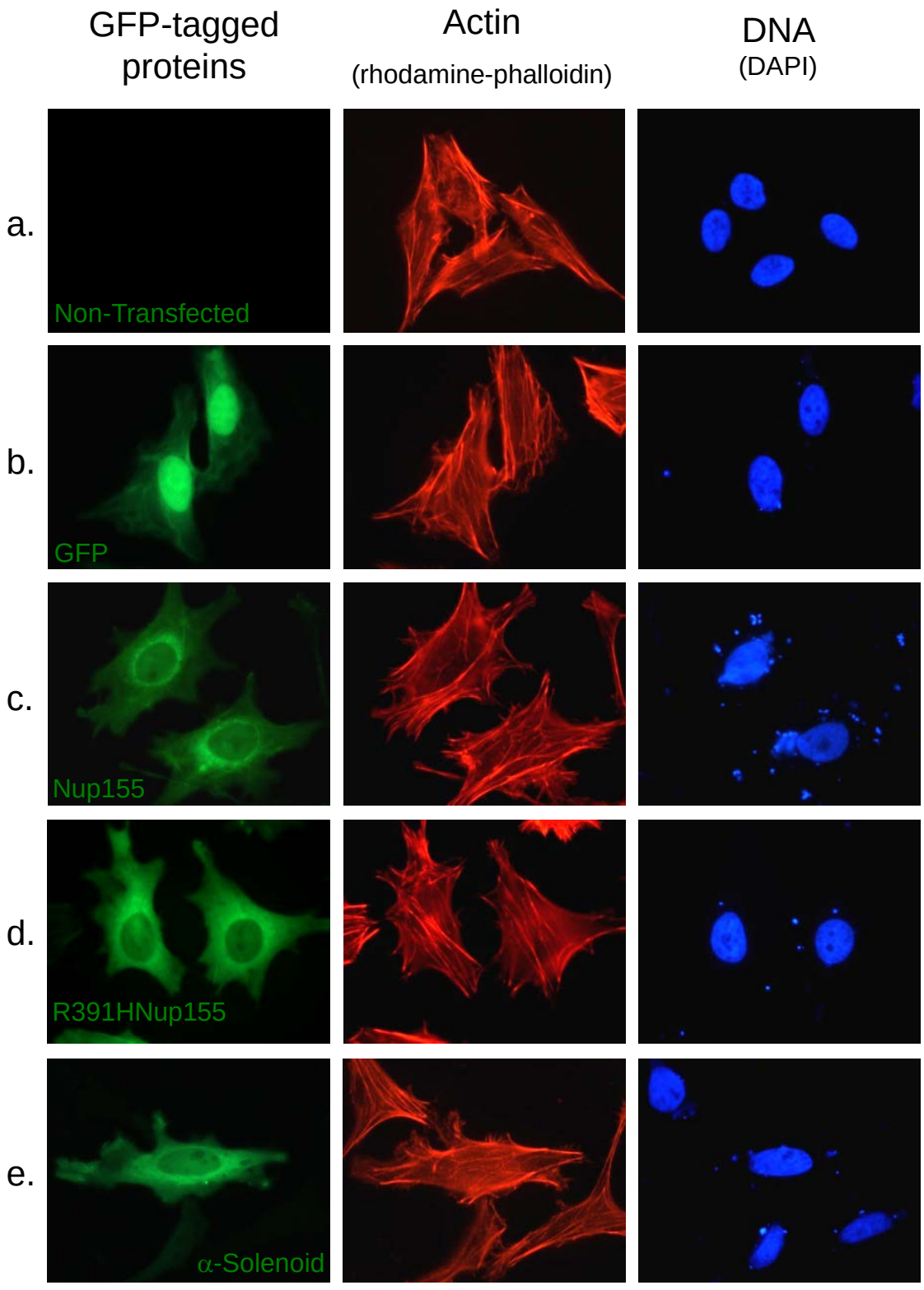
GFP-tagged proteins
Actin
(rhodamine-phalloidin)
DNA
(DAPI)
a.
Non-Transfected
b.
GFP
c.
Nup155
d.
R391HNup155
e.
α-Solenoid

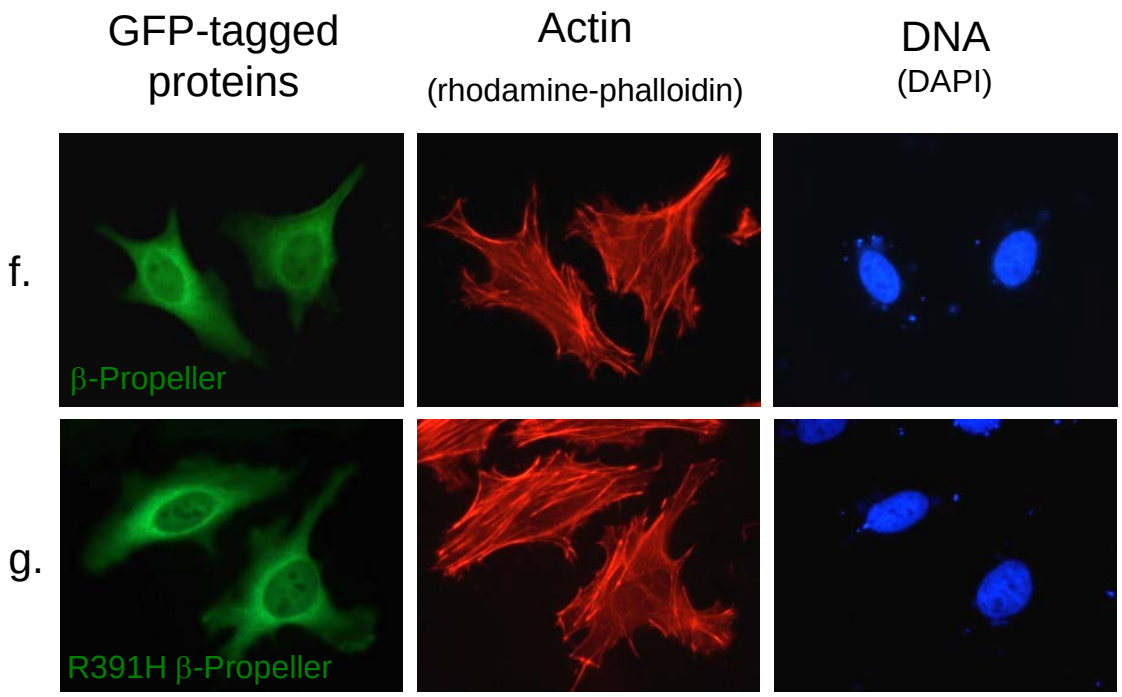

Figure 8, continued

Robinette *et al.*, 1996). For this we made use of the human osteosarcoma cell line U20S 2-6-3, which contains roughly 200 copies of a plasmid containing 256 repeats of the *lac* operator (LacO) inserted into a euchromatic region of chromosome 1 (Figure 9) (Janicki *et al.*, 2004). As the *lac* repressor (LacI) contains a DNA-binding domain that targets the LacI protein to the *lac* operator DNA sequence with high specificity, proteins of interest can be selectively localized to the LacO array (Figure 9). Here we created fusion proteins of the form LacI-CFP-Nup155.

For the purposes of this experiment, a plasmid of the form pSV2-LacI-CFP-hNup155 was constructed with the goal of using the LacI domain to anchor Nup155 to the LacO repeat site on chromosome 1. Following transient transfection, many copies of LacI-CFP-hNup155 bind to the LacO array, generally creating 1 bright focus when anti-LacI antibodies are added to pinpoint Nup155. The presence of any endogenous nucleoporins that bind to the localized Nup155 were determined by looking for co-localization of fluorescent antibodies to a Nup in question with the anti-LacI antibodies. Transfection of U20S 2-6-3 cells with LacI-CFP alone revealed a bright anti-LacI stained intranuclear site. However, this LacI site did not recruit any of the nucleoporins tested (Figure 10a, c, e, g, i, k, m, o, q). These negative controls show that none of the anti-nucleoporin antibodies bind non-specifically to a LacI-CFP construct.

Next, we looked at cells where a pSV2-LacI-CFP-hNup155 construct was transiently transfected into U20S 2-6-3 cells. We found that most of the nucleoporins tested for were not recruited to the Nup155 immobilized at the LacO

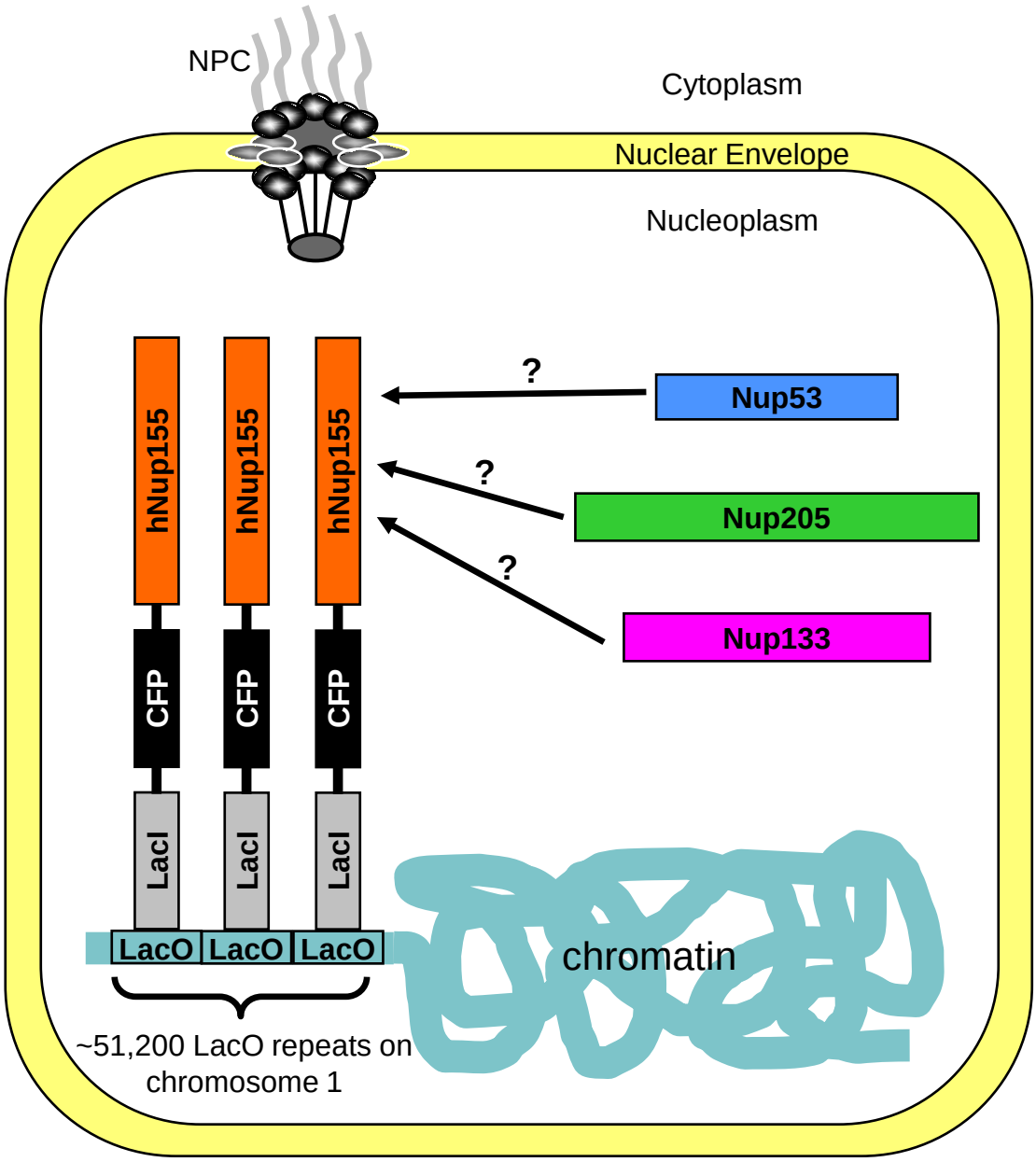

Figure 9 – The LacI – LacO Protein Binding Assay

Approximately 200 copies of the p3216PECMS2β plasmid was inserted into chromosome 1 to form the U20S 2-6-3 osteosarcoma cell line (Janicki *et al.* 2004). The original plasmid contains 256 repeats of the *lac* operator (LacO). Many copies of the LacI-CFP-hNup155 fusion protein are then expressed by transient transfection of the U20S 2-6-3 cells. Inside the nucleus, the DNA-binding LacI domain of LacI-CFP-hNup155 binds to the LacO DNA array. Next, fluorescently-labeled antibodies are used to detect the presence or absence of endogenously expressed nucleoporins co-localizing with the LacI-CFP-hNup155 *in vivo*.

Figure 10 - Nup53 and Pom121 are Recruited to Nup155 Immobilized on Chromatin

U20S 2-6-3 cells were transiently transfected with pSV2-LacI-CFP for control conditions or pSV2-LacI-CFP-hNup155 for experimental conditions. Mouse anti-LacI primary and FITC-labeled goat anti-mouse secondary antibodies yielded green labeling for LacI-containing constructs (second column). Nucleoporins were identified by rat primary antibodies against Nup155 (a and b), Nup53 (c and d), Nup62 (e and f), Nup93 (g and h), Nup98 (i and j), Nup133 (k and l), Nup160 (m and n), Nup214 (o and p), and Pom121 (q and r). Texas Red-labeled goat anti-rat secondary antibodies conferred red staining of these Nups (first column). Co-localization of red and green fluorescence yields yellow foci/patches that indicate likely protein interactions (third column). Nuclear DNA is demarcated by blue DAPI DNA stain (fourth column). None of the control LacI-CFP transfections (a, c, e, g, i, k, m, o, and q) showed Nup co-localization with LacI, indicating that these Nups do not non-specifically bind to LacI-CFP. Panel (b) verifies that Nup155 is in fact present in the LacI-CFP-Nup155 construct. Other nucleoporins that co-localized with and thus ostensibly bind to Nup155 were Nup53 (d) and Pom121 (r).

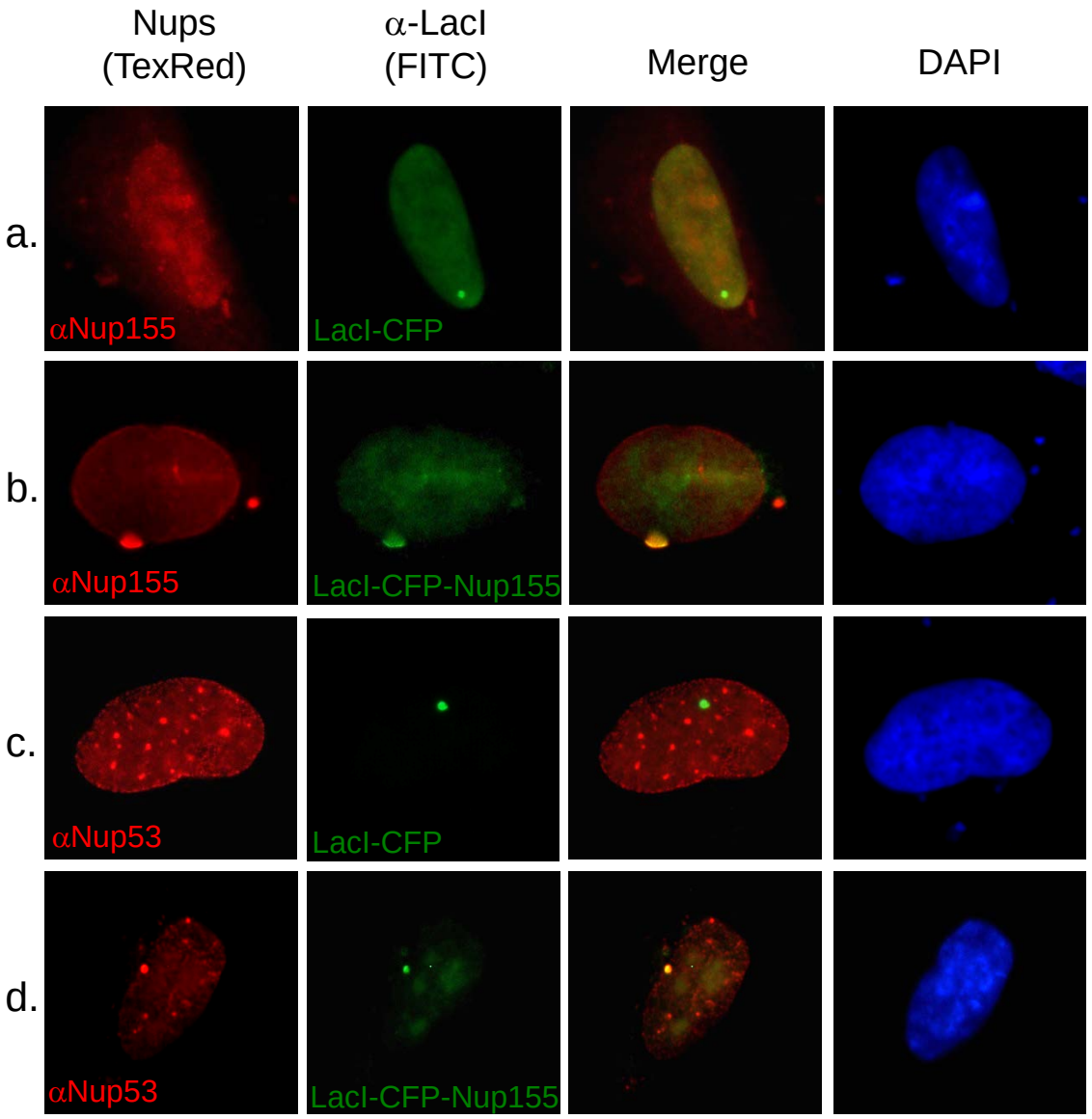
Nups
(TexRed)
α-LacI
(FITC)
Merge
DAPI
a.
αNup155
LacI-CFP
b.
αNup155
LacI-CFP-Nup155
c.
αNup53
LacI-CFP
d.
αNup53
LacI-CFP-Nup155

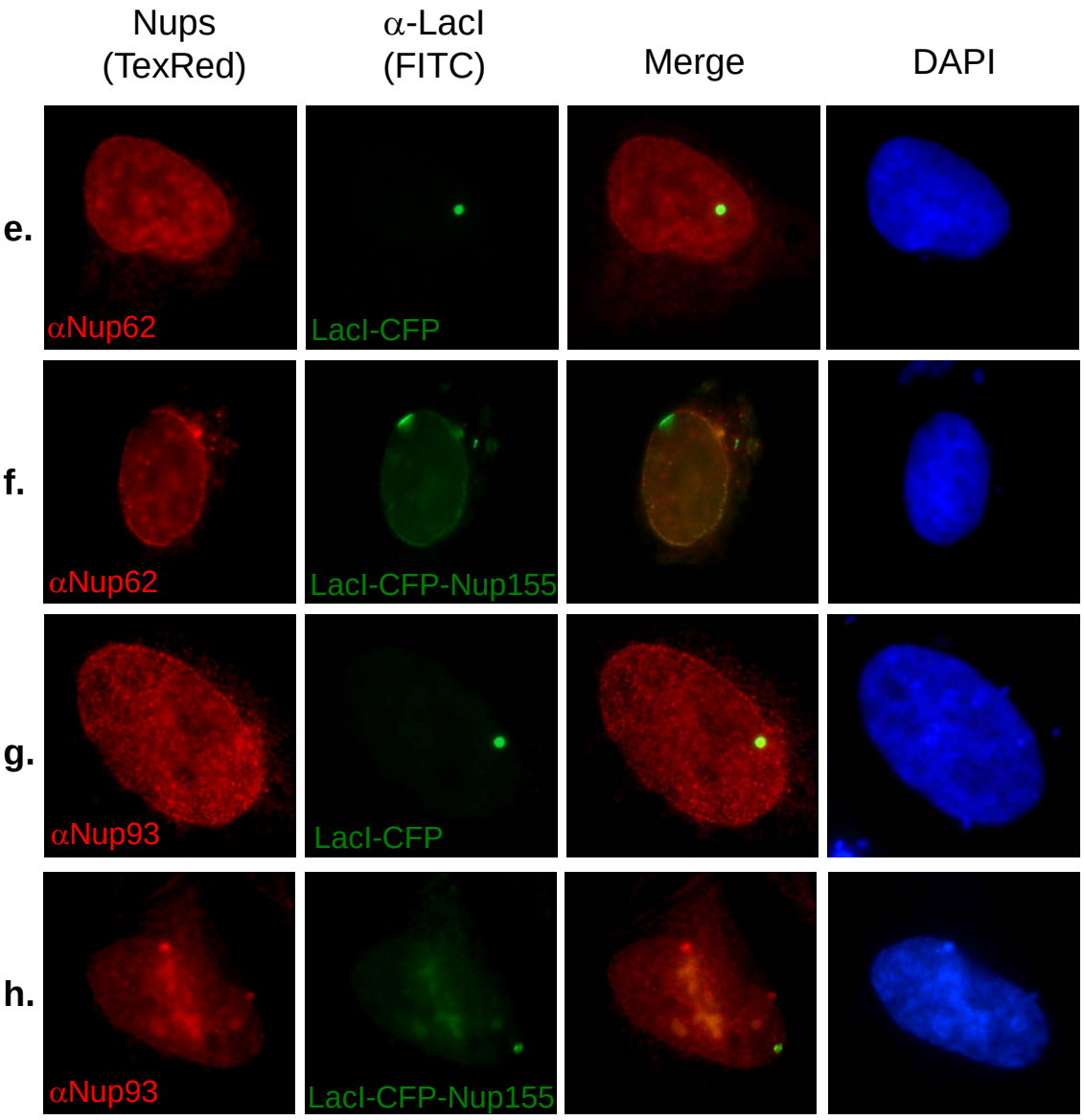

Figure 10, continued

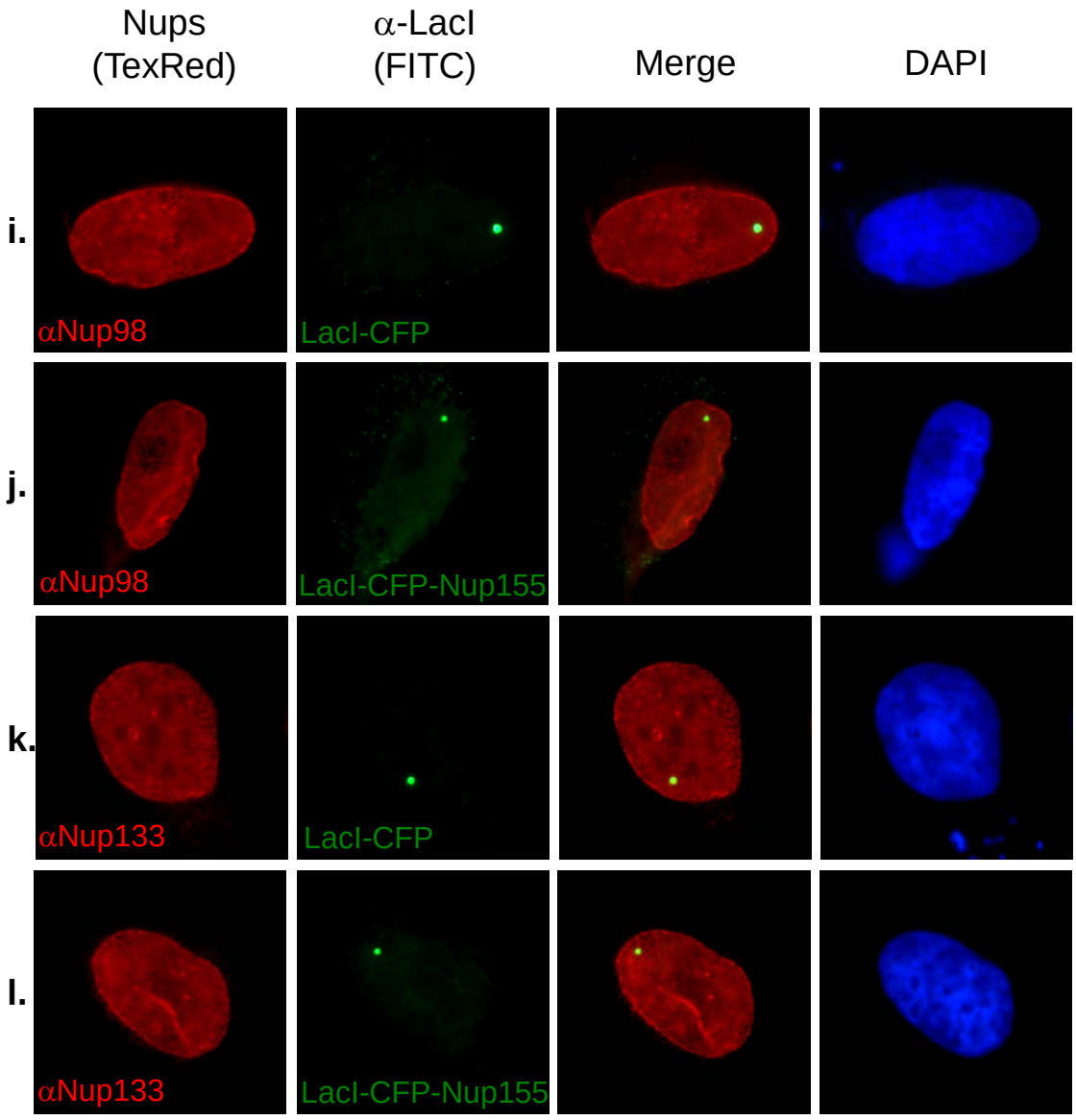

Figure 10, continued

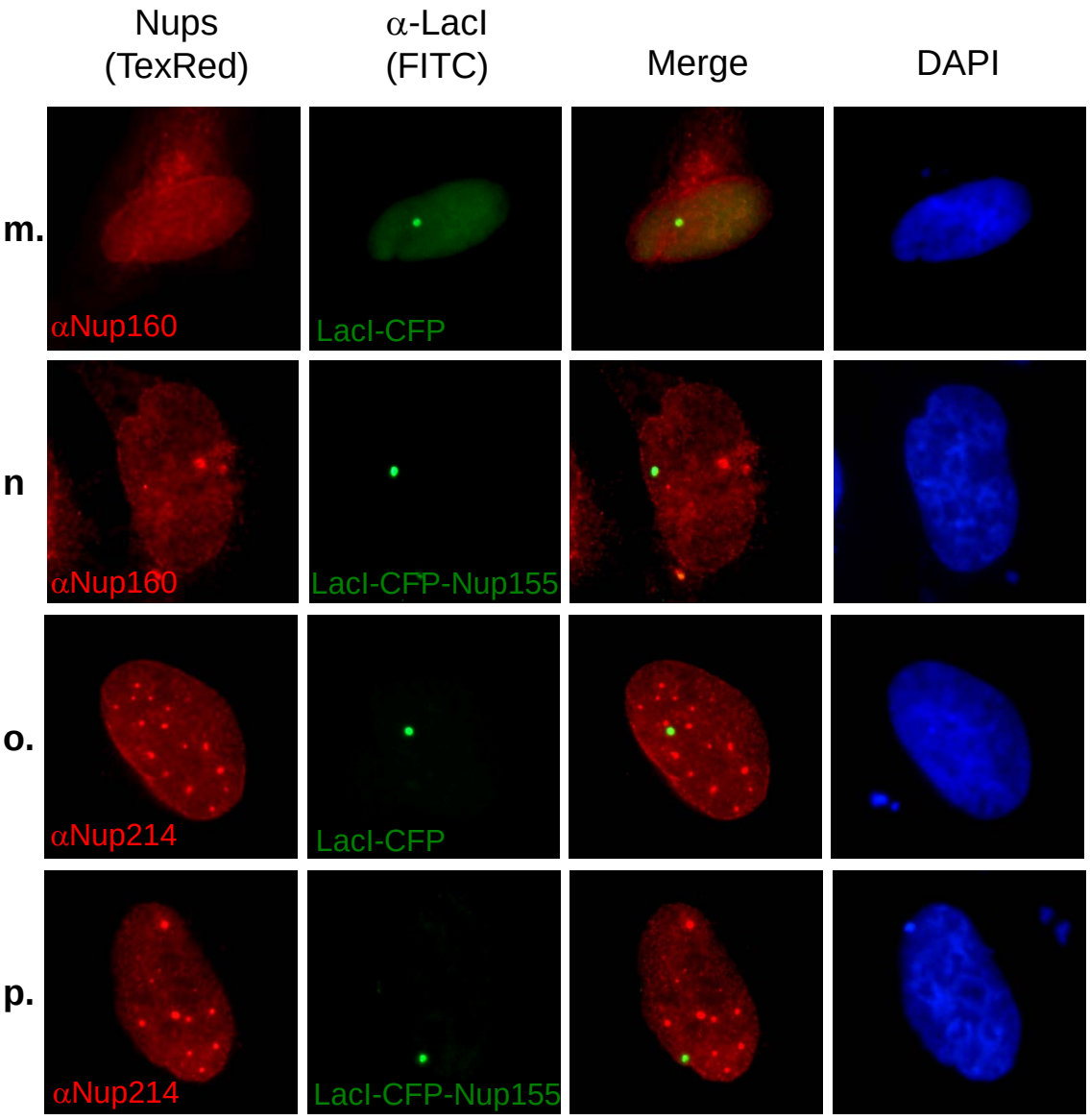

Figure 10, continued

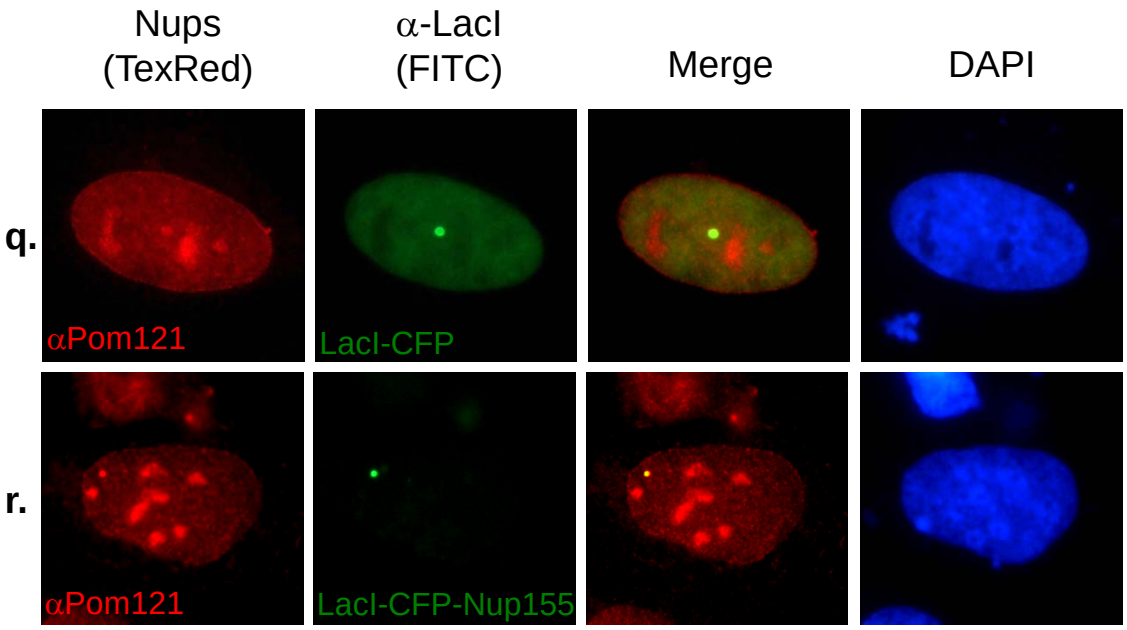

Figure 10, continued

intranuclear site. Nucleoporins absent from the LacI-CFP-Nup155-LacO array included Nup 62 (Figure 10f), Nup93 (Figure 10h), Nup98 (Figure 10j), Nup133 (Figure 10l), Nup160 (Figure 10n), and Nup214 (Figure 10p). On average, the aforementioned nucleoporins co-localized with the LacI-CFP-Nup155 in only 3.0 $\pm$ 0.6% of the cells observed.

As a positive control, anti-hNup155 antibody co-localized with the anti-LacI antibody 85.8 $\pm$ 2.0% in LacI-CFP-hNup155 transfected cells, indicating that Nup155 is correctly localized at the point of LacI fluorescence (Figure 10b; Figure 11). This can also be seen as a theoretical maximum for co-localization in this experiment. Specific nucleoporins were found to strongly co-localize with Nup155. These included Nup53 (54.5 $\pm$ 4.5% of $LacI^+$ cells) and the integral membrane nucleoporin Pom121 (65.6 $\pm$ 0.8% of $LacI^+$ cells)(Figure 10d, r; Figure 11). These values help to fortify an already strong argument in the literature for the association of Nup53 and Pom121 with Nup155. Their complete overlap indicated by co-localization, coupled with the close proximity of Nup53 and Pom121 to Nup155 within the context of the nuclear pore lends additional credence to their proposed binding.

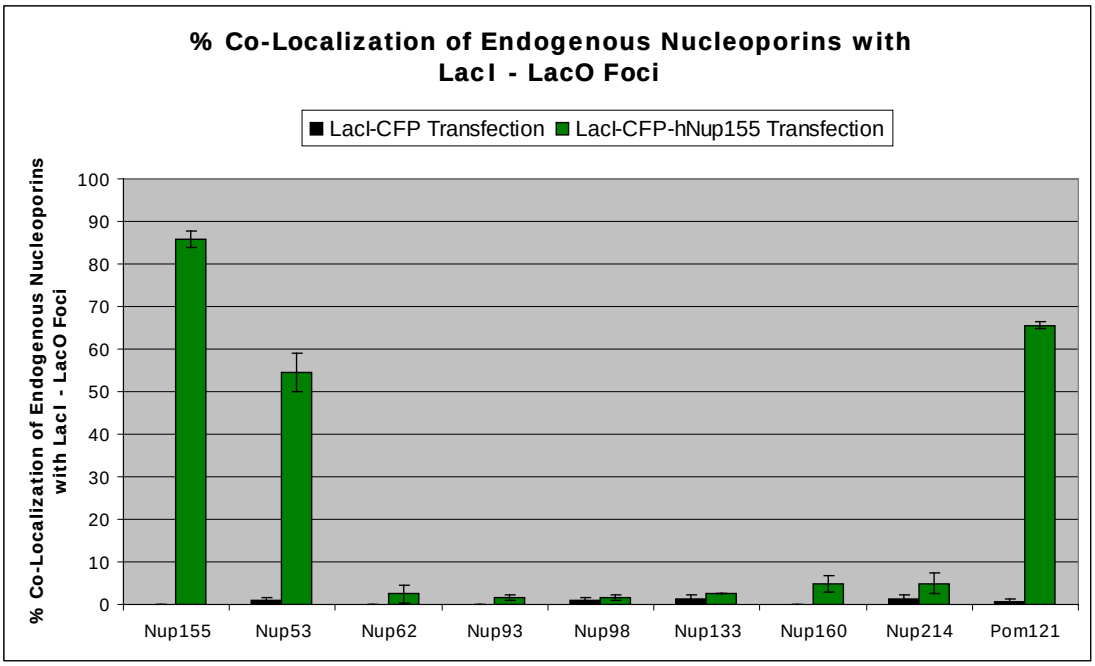

Figure 11 - Quantitation of Endogenous Nucleoporins Co-localizing with hNup155 Immobilized on Chromatin

U2OS 2-6-3 cells in Figure 10 were transiently transfected with LacI-CFP (negative control) or LacI-CFP-hNup155. Cells were assessed for co-localization between LacI – LacO foci and endogenous nucleoporins. The LacI – LacO foci were visualized with FITC-labeled goat anti-mouse secondary antibodies in green. The endogenous nucleoporins were visualized with Texas Red-labeled goat anti-rat secondary antibodies in red. Co-localization was defined as overlapping red and green secondary antibody labeled foci to produce yellow fluorescence. The wild type fluorescence pattern of certain endogenous nucleoporin such as Nup53, Nup62, Nup93, Nup160, Nup214, and Pom121 produce nucleoplasmic foci. To avoid false positive co-localization counts for these foci with LacI – LacO, only Nup staining patterns that conformed to the same shape, size, and location of the LacI fluorescence were counted as being positive for co-localization. At least 120 cells were counted for each condition. Green bars represent Nup co-localization with LacI-CFP-hNup155. Black bars are LacI-CFP controls, which show almost no co-localization with endogenous Nups. Strong co-localization is seen for 3 nucleoporins: Nup155, Nup53, and Pom121. Nup155 can be seen as a positive control and evidence that the Nup155 within the LacI-CFP-hNup155 construct is present and correctly localized. Nup53 and Pom121 co-localize with Nup155 to such an extent that a direct interaction between these proteins is likely. Error bars represent standard error.

DISCUSSION

The nuclear pore complex is a vast and diverse structure. Its many constituent parts carry out a broad array of cellular functions. Even its assembly takes on a variety of forms. During interphase, components of the pore are inserted into both sides of a continuous nuclear envelope. In mitosis, the nuclear envelope retracts into the ER and the soluble sub-complexes of the NPC dissociate and diffuse throughout the cytoplasm. After mitosis these sub-complexes must re-associate, anchor to chromatin, and promote the fusion of nascent nuclear envelopes. In order to make sense of the nuclear pore's complexity, it is advantageous to break this structure down and analyze its most basic elements: the nucleoporins. Going further, the functional domains of these nucleoporins can yield insight into their overall function. The same can be said for analysis of mutations, as loss of function can tell us equally much about what a protein is capable of. For all of the aforementioned reasons, an endeavor to dissect the function of Nup155 within the nuclear pore complex was undertaken.

Dissection of the Localization of Nup155

My endeavor began with the basic question of localization. I have demonstrated that full length Nup155 localizes to the nuclear rim, as is expected for all nucleoporins during interphase (Figure 3b). The same cannot be said for full length R391H Nup155 (Figure 3c) (Zhang *et al.*, 2008). This intriguing mutation has been shown to cause atrial fibrillation and heart attacks in both

mice and humans (Zhang *et al.*, 2008). It points to the essential nature of Nup155 and the fact that this mutant does not localize correctly is a first step in characterizing its cellular effects. The 2 functional domains of Nup155, the α-solenoid and β-propeller domains, were found to localize to the nuclear rim, albeit at lower levels when compared to the full length protein (Figure 3d, e). The nuclear rim localization of the β-propeller domain is lost when it contains the R391H mutation (Figure 3f). This data indicates that both the α-solenoid and β-propeller domains contribute to Nup155's correct localization and that this is lost as a result of the R391H mutation.

The β-propeller domain localization pattern that I observed is supported by recent findings which show that this domain anchors Nup155 to the nuclear pore through interactions with Nup93 and Nup53 (Busayavalasa *et at.*, 2012). In that same paper, the α-solenoid was found to bind to and direct the localization of the inner nuclear membrane proteins LBR and otefin to the nuclear rim. The same conclusion was drawn when HeLa cells depleted of Nup155 by RNAi failed to correctly localize the inner nuclear membrane proteins LBR, Lem2, and Lap2 to the nuclear rim (Mitchell *et al.*, 2010). Intriguingly, the α-solenoid domain localization at the nuclear rim shown here (Figure 3d) has not been previously observed. This could be a result of the α-solenoid domain interacting with the endogenous Nup155 β-propeller domain or inner nuclear membrane proteins.

Cardiac Considerations

If Nup155 is not anchored to the pore, then it cannot correctly interact with the necessary nucleoporins and also cannot direct the localization of the above inner nuclear membrane proteins. These defects could explain the cardiomyopathies, such as atrial fibrillation and early sudden cardiac death, observed by Zhang *et al.* (2008) in R391H humans and mice. Many cardiomyopathies have previously been associated with defective INM proteins. Humans with an R374H nesprin-1 mutation, as well as mice lacking the carboxy-terminal KASH domain of nesprin-1, both feature dilated cardiomyopathy with conduction system defects that are reminiscent of those found by Zhang *et al*. (2008) for Nup155$^{+/-}$ knockout mice (Puckelwartz *et al.*, 2010). Similarly, emerin mutations in humans have been shown to cause Emery-Dreifuss muscular dystrophy (Bione *et al.*, 1994). This condition leads to cardiomyopathy in the form of heart block, which manifests as a blockage in any of the electrical conduction systems of the heart (Bione *et al.*, 1994). If INM proteins are not localized correctly without functional Nup155, this may explain the cardiac deficiencies seen in the R391H mutants.

Poly[A]$^+$ mRNA Export

Once the groundwork of localization data was laid down, specific functional analyses of Nup155 were begun. Protein and RNA are the most common and essential cargoes transported through the nuclear pore complex, so the effects of Nup155 alteration on these trafficking events were assessed next.

As far as poly[A]$^+$ mRNA transport is concerned, overexpression of three Nup155 constructs were found to inhibit the nuclear export of cellular mRNA. These were full length R391H Nup155, the β-propeller domain, and the R391H β-propeller domain of Nup155 (Figure 4e, g, h; Figure 5). The β-propeller is the common thread in all of these conditions, likely indicating a dominant negative effect that is exacerbated by the R391H mutation.

The defect in poly[A]$^+$ mRNA export that we observe upon overexpression of mutant R391H Nup155, the β-propeller domain, or the R391H β-propeller domain can also be viewed in terms of Nup155's functional domains. The β-propeller has been shown to be essential for NPC anchoring and binding to Nups (Busayavalasa *et al.*, 2012, Mitchell *et al.*, 2010). This is supported by my finding that the R391H mutation in the β-propeller eliminated nuclear rim localization of Nup155 (Figure 3c, f). The β-propeller may cause inhibition of mRNA export by binding to the nuclear pores and preventing incorporation of full length wild type Nup155 during interphase and/or mitotic nuclear pore assembly. The mRNA export factor Gle1 is known to bind to the Nup155 α-solenoid domain (Rayala *et al.* 2004); thus, the relative absence of the α-solenoid domain in cells where excess β-propeller domain has replaced the full length protein could lead to an inability to export mRNA. In my study, poly[A]$^+$ mRNA was retained within the nucleus to the greatest extent when the constructs that contained a mutation in the β-propeller were transfected into cells (Figure 4e, h; Figure 5). It is possible that these R391H mutant proteins are exerting a dominant negative

effect on poly[A]$^+$ mRNA export by sequestering proteins necessary for RNA export. The fact that these R391H mutants are not localized at the NPC may enhance this deficit by leading to incorrect localization of the RNA export machinery.

Protein Import and Export Are Not Defective

When RGG protein import and export were examined, neither R391H nor wild type full-length Nup155 had any effect (Figure 7). If canonical protein transport is not being altered by overexpression of these proteins, then any other cellular deficits created by them must be resultant from different pathways. This demonstrates that the localization and poly[A]$^+$ mRNA deficits observed here are independent of nuclear import through the importin β pathway and of nuclear export through the Crm1/exportin-1 pathway. As importin β and exportin-1 are the 2 most prevalent pathways for nuclear protein import and nuclear protein export, respectively, our finding that neither wild type nor R391H Nup155 transfection had any effect on RGG protein transport was quite striking. It is also surprising that the inhibition of poly[A]$^+$ mRNA export is unrelated to these processes.

Nup155 lacks the FG-Nup repeats found in nucleoporins that interact with the karyopherins. RGG protein import is known to be mediated by the nuclear import receptor importin β (Henderson and Percipalle, 1997; Love *et al.*, 1998; Perkins *et al.* 1989). RGG protein export is known to be carried out by the nuclear export receptor Crm1/exportin-1 (Fornerod *et al.*, 1997, Love *et al.*,

1998). As these nuclear karyopherins mediate their movement through the nuclear pore by interacting with the FG-repeat nucleoporins, it might not be surprising that Nup155, which lacks FGs, does not have a role in trafficking of RGG protein cargo. However, Zhang *et al.* (2008) showed that R391H transfected HeLa cells are defective in the specialized transport pathway of Hsp70 protein nuclear import. A prime candidate for this pathway is through the nuclear import receptor Hikeshi, which has previously been shown to specifically mediate import of the ATP bound form of Hsp70s upon heat shock (Kose *et al.*, 2012). Our work demonstrates that general cellular protein import differs from heat shock protein import. Nup155 may thus have a differential role in the transport of different protein cargos.

Probing Protein-Protein Interactions *In Vivo* Using a LacI – LacO DNA Array System

The next step was to probe for Nup155 interactions with other nucleoporins. A novel system utilizing an *in vivo* assay was used to evaluate Nup155 binding in the native cellular environment. In this binding assay, hNup155 was found to recruit hNup53 (54.5 $\pm$ 4.5%) and hPom121 (65.6 $\pm$ 0.8%) (Figure 10d, r, Figure 11). A number of other nucleoporins did not co-localize with Nup155 (Figure 10f, h, j, l, n, p). When compared with the average frequency of these non-colocalizing protein constructs (3.0 $\pm$ 0.6%), I have strong evidence for Nup53 and Pom121 binding to Nup155 (Figure 11).

Nup155 binding to Nup53 has been seen *in vitro* in GST-Nup53 pulldowns of solubilized rat liver nuclear envelopes, in GST-Nup53 pulldowns of endogenous and truncated *Drosophila* Nup155, and in GST-xNup53 pulldowns from *E. coli* lysates overexpressing NusA-tagged xNup155 (Hawryluk-Gara *et al.*, 2005, Hawryluk-Gara *et al.*, 2008, Busayavalasa *et al.*, 2012, Eisenhardt *et al.*, 2013). Disruption of the Nup53-Nup155 binding by means of a K262A Nup53 mutation has been shown to inhibit the *in vitro* formation of a closed nuclear envelope and NPCs (Eisenhardt *et al.*, 2013). In that same *in vitro* study, the recruitment of Nup155, and subsequently Nup93 complex members followed by the Nup62 complex, was dependent on Nup155 binding to Nup53 (Eisenhardt *et al.*, 2013). A similar interaction has been observed between yeast Nup53 homologs (Nup53p and Nup59p) and yeast Nup155 homologs, such as Nup157p and Nup170p, using GST pulldowns from yeast extracts (Marelli *et al.*, 1998, Lusk *et al.*, 2002, Makhnevych *et al.*, 2003). The evidence provided in this study demonstrates specific Nup155 – Nup53 interaction *in vivo* in human cells for the first time.

The same can be said for the Pom121 – Nup155 interaction we observe with our *in vivo* reporter system. It previously has been demonstrated *in vitro* that GST-Pom121 binds to Nup155 in pulldowns of solubilized rat liver nuclear envelopes (Mitchell *et al.*, 2010). Likewise, GST-Nup155 was found capable of binding to recombinant Pom121 *in vitro* (Mitchell *et al.*, 2010). Similar results were found *in vitro* using *Xenopus* egg extracts where GST-Pom121 bound to Nup155 (Yavuz *et al.*, 2010). As Nup155 and Pom121 appear from the above to

be in close proximity to one another in the nuclear pore, the observed interaction is highly feasible and could serve to link the nuclear membrane to the nuclear pore.

It is intriguing that Nup155 was not seen by us to co-localize with Nup93. There is some evidence from GST-Nup93 pulldowns from HeLa cell lysates and from *Drosophila* extracts that Nup155 and Nup93 directly interact (Hawryluk-Gara *et al.*, 2005, Busayavalasa *et al.*, 2012). Even if these 2 Nups do not bind directly, as was suggested by Hawryluk-Gara *et al.,* 2008, there is strong evidence for them being in the same sub-complex (Hawryluk-Gara *et al.* 2005). This would lead one to theorize that Nup155 and Nup93 could still co-localize in our LacI – LacO *in vivo* system, but we did not see this. Perhaps the LacI-CFP fusion to the N-terminus of Nup155 disrupts interaction with Nup93.

Another Nup155 interaction that has been published is one with Nup62 (Yoshimura *et al*. 2013). Nup155 and Nup62 were shown to become covalently linked by a disulfide bond after the cell was exposed to oxidative stress (Yoshimura *et al*. 2013). Interestingly, immunoblotting of HeLa cell lysates revealed novel Nup155 containing bands that appeared upon hydrogen peroxide treatment and disappeared following Nup62 depletion by siRNA (Yoshimura *et al*. 2013). As the inner ring of the Nup93 complex, which contains Nup155, is adjacent to the FG-Nup-containing central structures of the pore that include Nup62, the interaction proposed is physically possible. Perhaps the LacI – LacO experimental setup does not reveal Nup62 – Nup155 interaction because oxidative stress has not been induced by us. In the future, it would be intriguing

to subject cells to an oxidizing agent and then perform the LacI – LacO binding assay to determine if oxidation can induce additional nucleoporin pairings.

One other interaction not assessed in our current study is that of Nup155 with the fusion protein Nup214-Abl1 that is present in the T-cell acute lymphoblastic leukemia cell line ALL-SIL (De Keersmaecker *et al.*, 2013). In that study, immunoprecipitation followed by mass spectrometry, as well as co-IP, demonstrated such a binding relationship (De Keersmaecker *et al.*, 2013). Interaction between Nup155 and a Nup214-Abl1 fusion protein that occurs exclusively in the non-physiological environment of an IP could explain why we do not see a Nup155 – Nup214 interaction in our *in vivo* system here. The difference in cell type between the studies may also play a role.

If Nup155 was able to bind a greater number of the nucleoporins tested, then it could be concluded that Nup155 is potentially capable of initiating nuclear pore complex assembly. Such a nucleoporin capable of seeding nuclear pores could be seen as the foundation upon which the NPC is built. The fact that Nup155 can only bind to 2 nucleoporins that are its relative neighbors within the context of the nuclear pore leads us to believe that instead it is a building block of the pore scaffolding.

Future Directions

This study of Nup155 has been revealing. Positive results obtained from localization, poly[A]$^{+}$ mRNA export, and nucleoporin binding experiments have expanded our knowledge of this protein and of the nuclear pore as a whole.

Even though Nup155 was not found to have an effect on importin β-mediated protein import, nuclear protein export mediated by exportin-1, or on microfilament structure, these findings also expand what is known by teaching us what this protein does not do. By no means is this a final or definitive study of Nup155 or the nuclear pore. Future work will continually add to our knowledge base. For instance, the LacI – LacO binding assay could in the future be performed with a variety of cell lines to determine the diversity of Nup155 binding.

The LacI – LacO NPC system could also be of value in probing other Nup155 functions. A number of nucleoporins serve other cellular functions in mitosis upon NPC disassembly. Our binding assay could be employed on cells synchronized in various stages of the cell cycle by chemicals such as lovastatin (G1), aphidicolin (S), or nocodazole (G2/M). Antibodies to known mitotic regulators could be tested for to determine differences in these phases. Strikingly, we reported the β-propeller domain and R391H mutations of Nup155 have an effect on poly[A]$^+$ mRNA export. Therefore, the LacI – LacO system could be used to probe for proteins which are involved in the mRNA export machinery that bind to Nup155. The α-solenoid domain has been shown by others to effect the localization of inner nuclear membrane proteins, so these could also be tested for co-localization with LacI-CFP-Nup155 or the LacI-CFP-α-solenoid *in vivo* at LacO DNA arrays (Busayavalasa *et at.*, 2012; Mitchell *et al.*, 2010).

The experiments on poly[A]$^+$ mRNA export, protein import and export, and microfilaments presented here were all performed by overexpressing Nup155.

Depletion of Nup155 by siRNA could yield additional insights into these experiments. Perhaps proteins involved in these processes are already saturated with Nup155 binding so that the elevated expression utilized in experiments here had little effect. If expression of Nup155 is artificially lowered, new phenotypes may emerge. Following siRNA depletion, the Nup155 constructs created could also then be transfected into the same cells. This could show us the effects of the Nup155 functional domains and mutations without the interference of endogenous Nup155.

A final powerful tool that could be used for future study of Nup155 is the *Xenopus* nuclear reconstitution system. This system can be used to assemble thousands of nuclei in a test tube by combining soluble protein and membrane fractions from *Xenopus laevis* eggs with *Xenopus* sperm chromatin and an ATP regeneration system. Because the final product of this assembly system are nuclei free from the confines of the cell, it is not difficult to add chemicals and proteins to directly visualize their effects. For example, various Nup155 constructs could be bacterially expressed, purified, and added into the system at different concentrations. Effects on nuclear assembly, nuclear membrane fusion, nuclear transport, and progression through mitosis could then be monitored. The effects of heat shock and oxidizing agents could also be easily assayed in a similar manner. This avenue of research was initially attempted by us, but ultimately abandoned as the purification of Nup155 could not overcome its insolubility. Perhaps novel techniques or the purification of functional domains or mutants could be more successful if given more time.

REFERENCES

Alber, F., Dokudovskaya, S., Veenhoff, L. M., Zhang, W., Kipper, J., Devos, D., Suprapto, A., Karni-Schmidt, O., Williams, R., Chait, B. T., Rout, M. P., Sali, A. (2007). Determining the architectures of macromolecular assemblies. Nature 450, 683-694.

Amberg, D. C., Goldstein, A. L., Cole, C. N. (1992). Isolation and characterization of RAT1: an essential gene of Saccharomyces cerevisiae required for the efficient nucleocytoplasmic trafficking of mRNA. Genes Dev 6, 1173-1189.

Bastos, R., Lin, A., Enarson, M., Burke, B. (1996). Targeting and function in mRNA export of nuclear pore complex protein Nup153. J Cell Biol 134, 1141–1156.

Bione, S., Maestrini, E., Rivella, S., Mancini, M., Regis, S., Romeo, G., Toniolo, D. (1994). Identification of a novel X-linked gene responsible for Emery-Dreifuss muscular dystrophy. Nat Genet 8, 323-327.

Bond, U. (2006). Stressed out! Effects of environmental stress on mRNA metabolism. FEMS Yeast Res 6, 160-170.

Busayavalasa, K., Chen, X., Farrants, A. K. Ö., Wagner, N., Sabri, N. (2012). The Nup155-mediated organization of inner nuclear membrane proteins is independent of Nup155 anchoring to the metazoan nuclear pore complex. J Cell Sci 125, 4214-4218.

Che, Y., Best, O. G., Zhong, L., Kaufman, K. L., Mactier, S., Raftery, M., Graves, L. M., Mulligan, S. P., Christopherson, R. I. (2013). Hsp90 inhibitor SNX-7081 dysregulates proteins involved with DNA repair and replication and the cell cycle in human chronic lymphocytic leukemia (CLL) cells. J Proteom Res 12, 1710-1722.

Cronshaw, J. M., Krutchinsky, A. N., Zhang, W., Chait, B. T., Matunis, M. J. (2002). Proteomic analysis of the mammalian nuclear pore complex. J Cell Biol 158, 915–927.

De Keersmaecker, K., Porcu, M., Cox, L., Girardi, T., Vandepoel, R., Op de Beeck, J., Gielen, O., Mentens, N., Bennett, K. L., Hantschel, O. (2013). NUP214-ABL1-mediated cell proliferation in T-cell acute lymphoblastic leukemia is dependent on the LCK kinase and various interacting proteins. Haematologica 99, 85-93.

Devos, D., Dokudovskaya, S., Williams, R., Alber, F., Eswar, N., Chait, B. T., Rout, M. P., Sali, A. (2006). Simple fold composition and modular architecture of the nuclear pore complex. Proc Natl Acad Sci U.S.A. 103, 2172-2177.

dos Remedios, C., Chhabra, D. (2008). Actin-binding proteins and disease. Prot Rev 8, 1-348.

Eisenhardt, N., Redolfi, J., Antonin, W. (2013). Nup53 interaction with Ndc1 and Nup155 are required for nuclear pore complex assembly. J Cell Sci, Epub ahead of print.

Flemming, D., Sarges, P., Stelter, P., Hellwig, A., Böttcher, B., Hurt, E. (2009). Two structurally distinct domains of the nucleoporin Nup170 cooperate to tether a subset of nucleoporins to nuclear pores. J Cell Biol 185, 387-395.

Fornerod, M., Ohno, M., Yoshida, M., Mattaj, I. W. (1997). CRM1 is an export receptor for leucine-rich nuclear export signals. Cell 90, 1051-1060.

Gallouzi, I. E., Brennan, C. M., Stenberg, M. G., Swanson, M. S., Eversole, A., Maizels, N., Steitz, J. A. (1999). HuR binding to cytoplasmic mRNA is perturbed by heat shock. Proc Natl Acad Sci U.S.A. 97, 3073-3078.

Heath, C. V., Copeland, C. S., Amberg, D. C., Priore, V. D., Snyder, M., Cole, C. N. (1995). Nuclear pore complex clustering and nuclear accumulation of poly(A)$^{+}$ RNA associated with mutation of the *Saccharomyces cerevisiae* RAT2/Nup120 gene. J Cell Biol 131, 1677–1697.

Henderson, B. R., Percipalle, P. (1997). Interactions between HIV Rev and nuclear import and export receptors: the Rev nuclear localization signal mediates specific binding to human importin-beta. J Mol Biol 274, 693-707.

Hertlein, E., Wagner, A. J., Jones, J., Lin, T. S., Maddocks, K. J., Towns, T. H., 3rd, Goettl, V. M., Zhang, X., Jarjoura, D., Raymond, C. A., West, D. A., Croce, C. M., Byrd, J. C., Johnson, A. J. (2010). 17-DMAG targets the nuclear facto-kappaB family of proteins to induce apoptosis in chronic lymphocytic leukemia: clinical implications of HSP90 inhibition. Blood 116, 45-53.

Huber, F., Schnauss, J., Rönicke, S., Rauch, P., Müller, K., Fütterer, C., Käs, J. (2013). Emergent complexity of the cytoskeleton: from single filaments to tissue. Adv Phys 62, 1-112.

Janicki, S. M., Tsukamoto, T., Salghetti, S. E., Tansey, W. P., Sachidanandam, R., Prasanth, K. V., Ried, T., Shav-Tal, Y., Bertrand, E., Singer, R. H., Spector, D. L. (2004). From silencing to gene expression: real-time analysis in single cells. Cell 116, 683-698.

Kendirgi, F., Rexer, D. J., Alcázar-Román, A. R., Onishko, H. M., Wente, S. R. (2005). Interaction between the shuttling mRNA export factor Gle1 and the nucleoporin hCG1: a conserved mechanism in the export of Hsp70 mRNA. Mol Biol Cell 16, 4304-4315.

Khose, S., Furuta, M., Imamoto, N. (2012). Hikeshi, a nuclear import carrier for Hsp70s, protects cells from heat shock-induced nuclear damage. Cell 149, 578-589.

Krebber, H., Taura, T., Lee, M. S., Silver, P. A. (1999). Uncoupling of the hnRNP Npl3p from mRNAs during the stress-induced block in mRNA export. Genes & Dev 13, 1994-2004.

Liu, Y., Liang, S., Tartakoff, A. M. (1996). Heat shock disassembles the nucleolus and inhibits nuclear protein import and poly(A)$^+$ RNA export. EMBO J 15, 6750-6757.

Love, D. C., Sweitzer, T. D., Hanover, J. A. (1998). Reconstitution of HIV-1 Rev nuclear export: independent requirements for nuclear import and export. Proc Natl Acad Sci USA 95, 10608-10613.

Lusk, C. P., Makhnevych, T., Marelli, M., Aitchison, J. D., Wozniak, R. W. (2002). Karyopherins in nuclear pore biogenesis: a role for Kap121p in the assembly of Nup53p into nuclear pore complexes. J Cell Biol 159, 267-278.

Makhnevych, T., Lusk, C. P., Anderson, A. M., Aitchison, J. D., Wozniak, R. W. (2003). Cell cycle regulated transport controlled by alterations in the nuclear pore complex. Cell 115, 813-823.

Marelli, M., Aitchison, J. D., Wozniak, R.W. (1998). Specific binding of the karyopherin Kap121p to a subunit of the nuclear pore complex containing Nup53p, Nup59p, and Nup170p. J Cell Biol 143, 1813-1830.

Mitchell, J. M., Mansfeld, J., Capitanio, J., Kutay, U., Wozniak, R. W. (2010). Pom121 links two essential subcomplexes of the nuclear pore complex core to the membrane. J Cell Biol 191, 505-521.

Natalizio, B. J., Wente, S. R. (2013). Postage for the messenger: designating routs for nuclear mRNA export. Trends Cell Biol 23, 365-373.

Perkins. A., Cochrane, A. W., Ruben, S. M., Rosen, C. A. (1989). Structural and functional characterization of the human immunodeficiency virus rev protein. J Acquir Immune Defic Syndr 2, 256-263.

Pritchard, C. E., Fornerod, M., Kasper, L. H., van Deursen, J. M. (1999). RAE1 is a shuttling mRNA export factor that binds to a GLEBS-like NUP98 motif at the nuclear pore complex through multiple domains. J Cell Biol 145, 237–254.

Puckelwartz, M. J., Kessler, E. J., Kim, G., DeWitt, M. M., Zhang, Y., Earley, J. U., Depreux, F. F. S., Holaska, J., Mewborn, S. K., Pytel, P., McNally, E. M. (2010). Nesprin-1 mutations in human and murine cardiomyopathy. J Mol Cell Cardiol 48, 600-608.

Radu, A., Blobel, G., Wozniak, R. W. (1993). Nup155 is a novel nuclear pore complex protein that contains neither repetitive sequence motifs nor reacts with WGA. J Cell Biol 121, 1–9.

Rayala, H. J., Kendirgi, F., Barry, D. M., Majerus, P. W., Wente, S. R. (2004). The mRNA export factor human Gle1 interacts with the nuclear pore complex protein Nup155. Mol Cell Proteomics 3, 145-155.

Robinette, C. C., Straight, A., Li, G., Willhelm, C., Sudlow, G., Murray, A., Belmont, A. S. (1996). In vivo localization of DNA sequences and visualization of large-scale chromatin organization using lac operator/repressor recognition. J Cell Biol 135, 1685-1700.

Rout, M. P., Aitchison, J. D., Suprapto, A., Hjertaas, K., Zhao, Y., Chait, B. T. (2000). The yeast nuclear pore complex: composition, architecture, and transport mechanism. J Cell Biol 148, 635-651.

Saavedra, C., Tung, K. S., Amberg, D. C., Hopper, A. K., Cole, C. N. (1996). Regulation of mRNA export in response to stress in Saccharomyces cerevisiae. Genes & Dev 10, 1608-1620.

Sadis, S., Hickey, E., Weber, L. A. (1988). Effect of heat shock on RNA metabolism in HeLa cells. J Cell Physiol 135, 377-386.

Skaggs, H. S., Xing, H., Wilkerson, D. C., Murphy, L. A., Hong, Y., Mayhew, C. N., Sarge, K. D. (2007). HSF1-TPR interaction facilitates export of stress-induced HSP70 mRNA. J Biol Chem 282, 33902-33907.

Stoffler, D., Fahrenkrog, B., Aebi, U. (1999). The nuclear pore complex: from molecular architecture to functional dynamics. Curr Opin Cell Biol 11, 391-401.

Tani, T., Derby, R. J., Hiraoka, Y., Spector, D. L. (1996). Nucleolar accumulation of poly(A)$^+$ RNA in heat-shocked yeast cells: implications of nucleolar involvement in mRNA transport. Mol Biol Cell 7, 173-192.

Tran, E. J., Wente, S. R. (2006). Dynamic nuclear pore complexes: life on the edge. Cell 125, 1041-1053.

Vasu, S., Shah, S., Orjalo, A., Park, M., Fischer, W. H., Forbes, D. J. (2001). Novel vertebrate nucleoporins Nup133 and Nup160 play a role in mRNA export. J Cell Biol 155, 339-353.

Watkins, J. L., Murphy, R., Emtage, J. L. T., Wente, S. R. (1998). The human homologue of *S. cerevisiae* Gle1p is required for poly(A)$^+$ RNA export. Proc Natl Acad Sci USA 95, 6779–6784.

Wolff, B., Sanglier, J. J., Wang, Y. (1997). Leptomycin B is an inhibitor of nuclear export: inhibition of nucleo-cytoplasmic translocation of the human immunodeficiency virus type 1 (HIV-1) Rev protein and Rev-dependent mRNA. Chem Biol 4, 139-147.

Yavuz, S., Santarella-Mellwig, R., Koch, B., Jaedicke, A., Mattaj, I. W., Antonin, W. (2010). NLS-mediated NPC functions of the nucleoporin Pom121. FEBS Lett 584, 3292-3298.

Zhang, X., Chen, S., Yoo, S., Chakrabarti, S., Zhang, T., Ke, T., Oberti, C., Yong, S. L., Fang, F., Li, L., de la Fuente, R., Wang, L., Chen, Q., Wang, Q.K. (2008). Mutation in nuclear pore component NUP155 leads to atrial fibrillation and early sudden cardiac death. Cell 135, 1017-1027.

Zheng, B., Han, M., Bernier, M., Wen, J. (2009). Nuclear actin and actin-binding proteins in the regulation of transcription and gene expression. FEBS J 276, 2669-2685.

Zhou, L. and Panté, N. (2010). The nucleoporin Nup153 maintains nuclear envelope architecture and is required for cell migration in tumor cells. FEBS Lett 584, 3013-3020.